Power law Stokes equations with threshold slip boundary conditions: Numerical methods and implementation

Jules Djoko K* Jonas Koko† Radek Kucera‡

November 27, 2018

Abstract

For the power law Stokes equations driven by nonlinear slip boundary conditions of friction type, we propose three iterative schemes based on augmented Lagrangian approach and interior point method to solve the finite element approximation associated to the continuous problem. We formulate the variational problem which in this case is a variational inequality and construct the weak solution of the continuous problem. Next, we formulate two alternating direction methods based on augmented Lagrangian formalism in order to separate the velocity from the symmetric part the velocity gradient and tangential part of the velocity. Thirdly, we present some salient points of a path-following variant of the interior point method associated to the finite element approximation of the problem. Some numerical experiments are performed to confirm the validity of the schemes and allow us to compare them.

Keywords: nonlinear Stokes, augmented Lagrangian, interior points method, alternating direction method of multiplier, simulations.

AMS Subject Classification: 65N30. 35J85

1 Introduction: nonlinear Stokes problem

The nonlinear Stokes problem arises in modeling flows of, e.g., biological fluids, lubricants, paints, polymer fluids where the fluid viscosity is assumed to be a nonlinear function of the fluid's velocity gradient tensor. A generalized nonlinear Stokes problem can be formulated as follows.

Find $(\boldsymbol{u}, p)$ such that

$$-\operatorname{div}\left(\nu(|D(\boldsymbol{u})|)D(\boldsymbol{u})\right) + \nabla p = \boldsymbol{f} \quad \text{in } \Omega, \tag{1.1}$$

$$\operatorname{div}\boldsymbol{u} = 0 \quad \text{in } \Omega, \tag{1.2}$$

where Ω, the flow region is a bounded domain in $\mathbb{R}^d$ with $d = 2, 3$. $\boldsymbol{u}(x)$ is the velocity vector, $p(x)$ stands for the pressure and $\boldsymbol{f} : \Omega \longrightarrow \mathbb{R}^d$ is the external force, assume to be in the dual space where the velocity is found. $|\cdot|$ denotes the Euclidean vector norm (that is $|\boldsymbol{u}|^2 = \boldsymbol{u} \cdot \boldsymbol{u}$) for a vector, whereas for a tensor of order two, it is the Frobenius norm. The symmetry part of the velocity gradient is

$$2D(\boldsymbol{u}) = \nabla\boldsymbol{u} + (\nabla\boldsymbol{u})^T.$$

The function $\nu(\cdot)$ describes the nonlinear kinematic viscosity coefficient of the fluid. In this paper, we consider the power law

$$\nu(|D(\boldsymbol{u})|) = \nu_0|D(\boldsymbol{u})|^{r-2}, \quad \nu_0 > 0,\ r > 1. \tag{1.3}$$

*Departement of Mathematics and Applied Mathematics, University of Pretoria, Private bag X20, Hatfield 0028, Pretoria, South Africa; Email: jules.djokokamdem@up.ac.za

†Clermont Université, LIMOS, UMR 6158 CNRS – Université Blaise Pascal, BP 10448, F-63000 Clermont-Ferrand, France; Email: jonas.koko@univ-bpclermont.fr

‡Department of Mathematics and Descriptive Geometry, Faculty of Mechanical Engineering and IT4Innovations National Supercomputing Center, VŠB - Technical University of Ostrava, 17. Listopadu 15/2172, 708 33 Ostrava, Czech Republic; Email: radek.kucera@vsb.cz

Note that for $r = 2$, (1.3) is constant, that is $\nu(|D(\boldsymbol{u})|) = \nu_0$ and (1.1) is reduced to the Stokes equation, a problem well investigated in [1]. When $1 < r < \infty$ (but $r \neq 2$), then (1.1) and (1.2) model an incompressible steady flow of a non-Newtonian viscous fluid of the power law type in an infinitely long cylinder of cross section Ω. It is observe that the law (1.3) is a particular case when one considers the White-Metzner type model for a visco-elastic fluid with the relaxation time considered to be zero.
The equations (1.1) and (1.2) are completed with boundary conditions. For that purpose, we assume that the boundary of Ω is partitioned into S and Γ, with $\overline{\partial\Omega} = \overline{S \cup \Gamma}$, and $S \cap \Gamma = \emptyset$. We consider homogeneous Dirichlet boundary condition on Γ, i.e.

$$\boldsymbol{u} = 0, \quad \text{on } \Gamma. \tag{1.4}$$

On S, we assume that the velocity is decomposed following its normal and tangential part as follows

$$\boldsymbol{u} = (\boldsymbol{u} \cdot \boldsymbol{n})\boldsymbol{n} + \boldsymbol{u}_{\boldsymbol{\tau}},$$

where $\boldsymbol{n}$ is the normal outward unit vector to S, and $\boldsymbol{u}_{\boldsymbol{\tau}}$ is parallel to the tangent direction $\boldsymbol{\tau}$. On S, we first assume the impermeability condition

$$\boldsymbol{u} \cdot \boldsymbol{n} = 0 \text{ on } S\ . \tag{1.5}$$

Now consider the Cauchy stress tensor $\boldsymbol{T} = -p\mathbb{I} + 2\nu_0|D(\boldsymbol{u})|^{r-2}D(\boldsymbol{u})$ and assume that the traction force $\boldsymbol{T}\boldsymbol{n}$ on S is decomposed as

$$\boldsymbol{T}\boldsymbol{n} = (\boldsymbol{T}\boldsymbol{n} \cdot \boldsymbol{n})\boldsymbol{n} + (\boldsymbol{T}\boldsymbol{n})_{\boldsymbol{\tau}}.$$

We impose on S the nonlinear slip boundary condition [2]

$$|(\boldsymbol{T}\boldsymbol{n})_{\boldsymbol{\tau}}| \leq g \quad \Rightarrow \quad \boldsymbol{u}_{\boldsymbol{\tau}} = \boldsymbol{0}, \tag{1.6}$$

$$|(\boldsymbol{T}\boldsymbol{n})_{\boldsymbol{\tau}}| > g \quad \Rightarrow \quad \boldsymbol{u}_{\boldsymbol{\tau}} \neq \boldsymbol{0}, (\boldsymbol{T}\boldsymbol{n})_{\boldsymbol{\tau}} = -(g + \kappa|\boldsymbol{u}_{\boldsymbol{\tau}}|)\frac{\boldsymbol{u}_{\boldsymbol{\tau}}}{|\boldsymbol{u}_{\boldsymbol{\tau}}|}, \tag{1.7}$$

where κ is a positive value, standing for the friction coefficient. $g : S \longrightarrow \mathbb{R}^+$ is the threshold function, non-negative. If $\kappa = 0$, the nonlinear slip boundary conditions (1.6)–(1.7) reduces to the classical Tresca friction law. It is worth mentioning that these conditions maybe be considered in the modeling of flow of polymer melts during extrusion (because in such problems, the part of the fluid that slips may depend on the tangential component of the stress on the boundary). In [3, 4], these conditions are used to model flows of yield stress fluids. We do not propose the non linear Stokes equations (1.1) with this boundary condition as a model for any real flow problem, because many others considerations should be taken into account; the geometry, the heat exchange, etc... We study this problem as a step towards constructing numerical tools for more some flow problems when the fluid slips at the boundary.
The goal of this work is to design reliable algorithms for the finite element approximation of the boundary value problem (1.1)...(1.7).
The partial differential equation describe by (1.1)...(1.7) is monotone elliptic and of nonlinear type, and the mathematical analysis of such problems has produced a large body of literature; let us mention among others, [5, 6, 7, 8] and the references therein. Many research works ([9, 10, 11, 12, 13, 14] just to cite a few) have dealt with the analysis and computations of fluid flow with Tresca's boundary conditions reported first in [7]. On the other hand and to our knowledge, the researchers in numerical analysis have ignored the situation with boundary conditions given by (1.6), (1.7) except the contributions [15, 16], in which Stokes and Navier Stokes are studied with two different solution strategies.

It is manifest that the problem (1.1)...(1.7) presents many numerical challenges among them; the nonlinear operator associated to the symmetric part of the velocity gradient, the incompressibility condition, the nontrivial boundary conditions (1.6) and (1.7) which brings a non-differentiable expression into the variational formulation. Mixed finite element approximation for the power law associated to Stokes equations together with Tresca's boundary conditions is considered in [17]. A priori error estimates analysis is derived and solution technique combining; regularization, penalization and operator splitting methods are formulated and implemented. Apart from the boundary conditions which by the way is a major modeling difference between the problem in [17] and the present one, the solution techniques we develop here are based on augmented Lagrangian algorithms, and interior point method. The friction boundary conditions

(1.6) and (1.7) complicate the variational formulation in the sense that the dissipation functional is of the form $J(\boldsymbol{u}, \boldsymbol{v})$, hence a careful choice of Lagrange multiplier(s) to relax the augmented Lagrangian functional is crucial. It is worth mentioning that one of the first works dedicated to the discretization and analysis of the elliptic equation with the nonlinearity (1.3) and Dirichlet boundary conditions goes back to the contribution of Glowinski and Marrocco in the seventies [18] in which a priori error analysis is proposed together with a complete derivation and analysis of solution technique based on an augmented Lagrangian approach. Having in mind the desire to separate the velocity from the velocity gradient, Glowinski and Marrocco have proposed an algorithm based on an alternative direction method of multiplier reducing the vectorial non-linear problem into a sequence composed of algebraic non-linear equation and linear system of equations. The problem we have in hand differs due to the friction boundary conditions (1.6) and (1.7). Indeed in our work there is a need to separate the velocity from the tangential part of the velocity and the symmetric part of the velocity gradient. It is important to note that some efforts have been made in [19, 20, 21, 22, 23, 24, 25] for the analysis of the convergence of the finite element discretzation of elliptic problems with the nonlinearity (1.3) and the Dirichlet boundary conditions. This work does not investigate a priori error control as this can be done following closely [17, 18, 19, 20, 21, 22, 23, 24, 25].
Some achievements in our work are reported in Section 3, Section 4 and Section 5 where detailed efficient algorithms are formulated and conditions under which iterative finite element solution converges are made clear. For the presentation of the alternative direction methods of multiplier(s) based on augmented Lagrange approach, we follow [26, 27]. The path following algorithm discussed here is a variant of the interior point method originally designed for problems in solid mechanics (see [28]). The three iterative schemes discussed in this work make use of Lagrange multipliers with the common goal of "softening" the difficulties by introducing new unknowns. The convergence analysis of the alternating direction of multipliers discussed can be done following the techniques presented in [26, 27], while the key points of the convergence concerning the interior point algorithm are discussed in Section 5. The rest of the paper is organized as follows:

- Section 2 is concerned with the weak formulation and the construction of weak solutions.
- Section 3 is devoted to the construction of numerical algorithm using the alternating direction method when one is interested in separating the velocity and the symmetric part of the velocity gradient.
- Section 4 is devoted to the construction of numerical algorithm using the alternating direction method when one is interested in separating the velocity, the symmetric part of the velocity gradient and the tangential part of the velocity.
- Section 5 describes the algorithm using the interior point method, with special attention given to the velocity.
- Section 6 is devoted to numerical results, discussions and conclusions.

2 Analysis of the continuous problem

In this section we formulate the variational formulation associated with the nonlinear problem (1.1)...(1.7), and introduce some notations and crucial properties which will be exploited throughout. The preliminaries materials are borrowed from [29, 30]. For $1 \leq p < \infty$; the Lebesgue space is

$$L^p(\Omega) = \left\{ v : \Omega \longrightarrow \mathbb{R};\ v \text{ is measurable and } \int_\Omega |v(\boldsymbol{x})|^p dx \leq \infty \right\},$$

with associated norm

$$\|v\|^p_{L^p(\Omega)} = \int_\Omega |v(\boldsymbol{x})|^p dx$$

for which it is a Banach space. And for the special case $p = 2$, it is a Hilbert space with the norm that will be denoted by $\|\cdot\|$. Finally when $p = \infty$ one has

$$L^\infty(\Omega) = \left\{ v : \Omega \longrightarrow \mathbb{R}, \;\middle|\; \begin{array}{l} \text{is measurable and there is a constant } c \\ \text{such that } |v(\boldsymbol{x})| \leq c \text{ a.e. on } \Omega \end{array} \right\},$$

with associated norm

$$\|v\|_{L^\infty(\Omega)} = \|v\|_\infty = \inf \{ c\ ;\ \ |v(\boldsymbol{x})| \leq c \ \text{ a.e. on } \Omega \}\ .$$

For any non-negative integer m and real number $p \geq 1$, we defined the Sobolev space

$$W^{m,p}(\Omega) = \{v \in L^p(\Omega) \ , \ \ \partial^\alpha v \in L^p(\Omega) \text{ for all } |\alpha| \leq m\},$$

where $\alpha = (\alpha_1, ..., \alpha_d)$ is the multi-index with $|\alpha| = \alpha_1 + \cdots + \alpha_d$, and $D^\alpha v$ the distributional derivative of v defined by

$$\partial^\alpha v = \frac{\partial^{|\alpha|} v}{\partial x_1^{\alpha_1} \cdots \partial x_d^{\alpha_d}} \ .$$

The space $W^{m,p}(\Omega)$ is equipped with the semi-norm and norm

$$|v|_{m,p}^r = \sum_{|\alpha|=m} \int_\Omega |D^\alpha v(\boldsymbol{x})|^p dx \quad , \quad \|v\|_{m,r}^p = \sum_{0 \leq |\alpha| \leq m} \int_\Omega |D^\alpha v(\boldsymbol{x})|^p dx \ .$$

The duality between, say, E and E' is denoted as $\langle \cdot, \cdot \rangle$. Throughout this work, boldface characters denote vector quantities, and $\boldsymbol{L}^r(\Omega) = L^r(\Omega)^d$ and $\boldsymbol{W}^{m,r}(\Omega) = W^{m,r}(\Omega)^d$, etc...

In order to introduce other functions spaces for the analysis of the boundary value problem (1.1)...(1.7), we take in a naive way the dot product between (1.1) and $\boldsymbol{u}$ and integrate the resulting equation over Ω. After utilization of the Green's formula and boundary conditions we arrived at

$$2\nu_0 \int_\Omega |D(\boldsymbol{u})|^r dx + \int_S g|\boldsymbol{u_\tau}| d\sigma + \kappa \int_S |\boldsymbol{u_\tau}|^2 d\sigma - \int_\Omega p \operatorname{div} \boldsymbol{u} dx = \langle \boldsymbol{f}, \boldsymbol{u} \rangle \ , \tag{2.1}$$

with $d\sigma$ being the surface measure associated to S. In this work, we assume once and for all that $g \in L^\infty(S)$. It is manifest from (2.1) that for the velocity one needs $\boldsymbol{u} \in \boldsymbol{W}^{1,r}(\Omega)$, and $\boldsymbol{u_\tau} \in \boldsymbol{L}^2(S)$. Hence we define the space

$$\boldsymbol{V} \ = \ \left\{ \ \boldsymbol{v} \mid \ \ \boldsymbol{v} \in \boldsymbol{W}^{1,r}(\Omega) \ , \ \boldsymbol{v_\tau} \in \boldsymbol{L}^2(S), \text{ and } \ \ \boldsymbol{v}|_\Gamma = \boldsymbol{0} \ , \ \boldsymbol{v}_n|_S = 0 \right\} .$$

Remark 2.1. *It should be noted that for $\boldsymbol{v} \in \boldsymbol{W}^{1,r}(\Omega)$, $\boldsymbol{v}|_{\partial\Omega}$ belong to $\boldsymbol{W}^{1-1/r,r}(\partial\Omega)$ which is not necessarily a subset of $\boldsymbol{L}^2(\partial\Omega)$.*

On the space $\boldsymbol{V}$ one considers the norm

$$|||\boldsymbol{v}|||^2 = \|\boldsymbol{v}\|_{1,r}^2 + \|\boldsymbol{v_\tau}\|_{L^2(S)}^2$$

for which it is a Banach space. Now a fractional Sobolev result in [29] (Theorem 7.58, p. 218) or ([5], p. 170) asserts that; if $\Omega \subset \mathbb{R}^d$ open bounded with $\mathcal{C}^1$ boundary $\partial\Omega$ then

$$W^{1-1/r,r}(\partial\Omega) \subset L^2(\partial\Omega) \quad \text{ for } \ 2d/(d+1) \leq r < 2 \ . \tag{2.2}$$

Hence we deduce that

Lemma 2.1. *There exists c such that for $2d/(d+1) \leq r < \infty$*

$$\|\boldsymbol{v}\|_{1,r}^2 \leq |||\boldsymbol{v}|||^2 \leq c\|\boldsymbol{v}\|_{1,r}^2 \ \ \textit{for all} \ \ \boldsymbol{v} \in \boldsymbol{V} \ .$$

Proof. By definition $\|\boldsymbol{v}\|_{1,r}^2 \leq |||\boldsymbol{v}|||^2$. To conclude the proof, we need to show that $\|\boldsymbol{v_\tau}\|_S$ is bounded above by $\|\boldsymbol{v}\|_{1,r}$.
For $r \geq 2$, one has $W^{1-1/r,r}(\partial\Omega) \subset L^r(\partial\Omega) \subset L^2(\partial\Omega)$, together with the theorem of trace leads to

$$\|\boldsymbol{v_\tau}\|_{L^2(S)}^2 = \|\boldsymbol{v}\|_{L^2(S)}^2 \leq c\|\boldsymbol{v}\|_{W^{1-1/r,r}(S)}^2 \leq c\|\boldsymbol{v}\|_{1,r}^2 \, .$$

Next, for $2d/(d+1) \leq r \leq 2$, we consider (2.2) and the theorem of trace to deduce that

$$\|\boldsymbol{v_\tau}\|_{L^2(S)}^2 = \|\boldsymbol{v}\|_{L^2(S)}^2 \leq c\|\boldsymbol{v}\|_{W^{1-1/r,r}(S)}^2 \leq c\|\boldsymbol{v}\|_{1,r}^2 \, .$$

□

Remark 2.2. *For $1 < r < 2d/(d+1)$, the norm $|||\cdot|||$ is not equivalent to the $W^{1,r}$-norm on $\boldsymbol{V}$, but for $2d/(d+1) < r < \infty$, the space $\boldsymbol{V}$ will be equipped with $W^{1,r}$-norm.*

Next, as far as the space of pressure is concerned, from (2.1) one observes that the pressure p should belong to $L^{r'}(\Omega)$, with r' the conjugate of r, that is $\frac{1}{r'}+\frac{1}{r}=1$. But in $L^{r'}(\Omega)$, the pressure is obtained up to a constant. Thus in order to eliminate the constant we define the space

$$M \quad = \quad L_0^{r'}(\Omega) = \left\{ p \mid \ p \in L^{r'}(\Omega) : \quad \int_\Omega p\, dx = 0 \right\},$$

with is a Banach space equipped with the norm $\|\cdot\|_{L^{r'}(\Omega)}$. With the spaces $\boldsymbol{V}$ and M, one can introduce the weak formulation of the boundary value problem (1.1)...(1.7).
We multiply (1.2) by $q \in L^{r'}(\Omega)$ and integrate over Ω. We take the dot product between (1.1) and $\boldsymbol{v}-\boldsymbol{u}$ with $\boldsymbol{v} \in \boldsymbol{V}$, integrate the resulting equation over Ω, apply Green's formula, and the boundary conditions (1.4), (1.5), (1.6) and (1.7) we obtain, for $\boldsymbol{f} \in \boldsymbol{V}' \equiv$ dual space of $\boldsymbol{V}$:

Find $(\boldsymbol{u}, p) \in \boldsymbol{V} \times M$ such that for all $(\boldsymbol{v}, q) \in \boldsymbol{V} \times M$

$$\langle A\boldsymbol{u}, \boldsymbol{v}-\boldsymbol{u}\rangle + b(\boldsymbol{v}-\boldsymbol{u}, p) + j_1(\boldsymbol{u}, \boldsymbol{v}) - j_1(\boldsymbol{u}, \boldsymbol{u}) \quad \geq \quad \langle \boldsymbol{f}, \boldsymbol{v}-\boldsymbol{u}\rangle, \tag{2.3}$$

$$b(\boldsymbol{u}, q) \quad = \quad 0 \tag{2.4}$$

with

$$\begin{aligned} \langle A\boldsymbol{u}, \boldsymbol{v}\rangle \quad &= \quad 2\nu_0 \int_\Omega |D(\boldsymbol{u})|^{r-2} D(\boldsymbol{u}) : D(\boldsymbol{v}) dx, \\ b(\boldsymbol{v}, q) \quad &= \quad -\int_\Omega q \,\mathrm{div}\, \boldsymbol{v} dx, \\ j_1(\boldsymbol{u}, \boldsymbol{v}) \quad &= \quad \int_S (g + \kappa|\boldsymbol{u}_{\boldsymbol{\tau}}|)|\boldsymbol{v}_{\boldsymbol{\tau}}|\, d\sigma\,, \end{aligned} \tag{2.5}$$

with $\boldsymbol{A} : \boldsymbol{B} = \sum\limits_{1\leq i,j\leq d} A_{ij}B_{ij}$. Note that the operators defined via (2.5) are well defined for $\boldsymbol{u}, \boldsymbol{v}$ in $\boldsymbol{V}$ and $q \in L^{r'}(\Omega)$. One important space when studying mixed formulations is being able to find the kernel of the bilinear form defined in different spaces. In this case we are talking about the kernel of $b(\cdot,\cdot)$ in $\boldsymbol{V}$ which is defined as follows

$$\boldsymbol{V}_{\mathrm{div}} = \left\{ \boldsymbol{v} \in \boldsymbol{V} : \quad b(\boldsymbol{v}, q) = 0 \ \ \forall q \in L^{r'}(\Omega) \right\},$$

and characterized by

$$\boldsymbol{V}_{\mathrm{div}} = \{ \boldsymbol{v} \in \boldsymbol{V} \ : \quad \mathrm{div}\, \boldsymbol{v}|_\Omega = 0 \ \}.$$

One easily check that $b(\cdot,\cdot)$ is continuous; that is

$$\text{for all} \ \ (\boldsymbol{v}, q) \in \boldsymbol{V} \times L^{r'}(\Omega) \ \ , \quad b(\boldsymbol{v}, q) \leq \|\boldsymbol{v}\|_{1,r} \|q\|_{L^{r'}(\Omega)}\,.$$

With the space $\boldsymbol{V}_{\mathrm{div}}$, we observe that (2.3)-(2.4) is equivalent to (see [21]): Find $\boldsymbol{u} \in \boldsymbol{V}_{\mathrm{div}}$ such that for all $\boldsymbol{v} \in \boldsymbol{V}_{\mathrm{div}}$

$$\langle A\boldsymbol{u}, \boldsymbol{v}-\boldsymbol{u}\rangle + j_1(\boldsymbol{u}, \boldsymbol{v}) - j_1(\boldsymbol{u}, \boldsymbol{u}) \geq \langle \boldsymbol{f}, \boldsymbol{v}-\boldsymbol{u}\rangle\,. \tag{2.6}$$

For the existence and uniqueness of solution of (2.6), we recall or introduce the monotonicity and continuity of A obtained in [5, 23, 25] which states that;

Lemma 2.2. *There exist positive constants $\alpha = \alpha(r,d)$ and $\beta = \beta(r,d)$, such that the following inequalities hold:*
If $r \in (1,2)$, then for all $\boldsymbol{u}, \boldsymbol{v}$ in $\boldsymbol{W}^{1,r}(\Omega)$,

$$\begin{aligned} \alpha\|\boldsymbol{u}-\boldsymbol{v}\|_{1,r}^2 \quad &\leq \quad \langle A\boldsymbol{u} - A\boldsymbol{v}, \boldsymbol{u}-\boldsymbol{v}\rangle \left(\|\boldsymbol{u}\|_{1,r} + \|\boldsymbol{v}\|_{1,r}\right)^{2-r}, \\ \|A\boldsymbol{u} - A\boldsymbol{v}\|_{-1,r'} \quad &\leq \quad \beta\|\boldsymbol{u}-\boldsymbol{v}\|_{1,r}^{r-1}. \end{aligned}$$

If $r \in (2,\infty)$, then for all $\boldsymbol{u}, \boldsymbol{v}$ in $\boldsymbol{W}^{1,r}(\Omega)$,

$$\begin{aligned} \alpha\|\boldsymbol{u}-\boldsymbol{v}\|_{1,r}^r \quad &\leq \quad \langle A\boldsymbol{u} - A\boldsymbol{v}, \boldsymbol{u}-\boldsymbol{v}\rangle, \\ \|A\boldsymbol{u} - A\boldsymbol{v}\|_{-1,r'} \quad &\leq \quad \beta\|\boldsymbol{u}-\boldsymbol{v}\|_{1,r} \left(\|\boldsymbol{u}\|_{1,r} + \|\boldsymbol{v}\|_{1,r}\right)^{r-2}. \end{aligned}$$

Thus from Lemma 2.2, we deduce that

Corollary 2.1. *Let $2d/(d+1) \leq r < \infty$, the operator $A : \boldsymbol{V} \longrightarrow \boldsymbol{V}'$ satisfy the following properties*

(1) There is a positive constant c such that for all $\boldsymbol{v} \in \boldsymbol{V}$, $\|A\boldsymbol{v}\|_{-1,r'} \leq c\|\boldsymbol{v}\|_{1,r}^{r-1}$ and A is hemi-continuous on $\boldsymbol{V}$, that is for all $\boldsymbol{v}, \boldsymbol{w}, \boldsymbol{u}$ in $\boldsymbol{V}$, the mapping $t \longrightarrow \langle A(\boldsymbol{u}+t\boldsymbol{v}), \boldsymbol{w}\rangle$ is continuous on $\mathbb{R}$.

(2) A is monotone meaning that for all $\boldsymbol{v}, \boldsymbol{w}$ in $\boldsymbol{V}$, $\langle A(\boldsymbol{v}) - A(\boldsymbol{w}), \boldsymbol{v}-\boldsymbol{w}\rangle \geq 0$.

(3) There is $\alpha > 0$ such that for all $\boldsymbol{v}$ in $\boldsymbol{V}$, $\langle A\boldsymbol{v}, \boldsymbol{v}\rangle \geq \alpha\|\boldsymbol{v}\|_{1,r}^r$.

The next result is important for the existence and uniqueness of solution of (2.6).

Lemma 2.3. *Let $\Omega \subset \mathbb{R}^d$ with $1 < r < \infty$. Let $\boldsymbol{v}_1, \boldsymbol{v}_2, \boldsymbol{w}_1, \boldsymbol{w}_2 \in \boldsymbol{V}$, then there exists c such that*

$$j_1(\boldsymbol{v}_1, \boldsymbol{w}_2) - j_1(\boldsymbol{v}_1, \boldsymbol{w}_1) + j_1(\boldsymbol{v}_2, \boldsymbol{w}_1) - j_1(\boldsymbol{v}_2, \boldsymbol{w}_2) \leq \begin{cases} \kappa|||\boldsymbol{v}_1 - \boldsymbol{v}_2||| \, |||\boldsymbol{w}_1 - \boldsymbol{w}_2||| & \text{if } 1 < r < 2d/(d+1) \\ \kappa c||\boldsymbol{v}_1 - \boldsymbol{v}_2||_{1,r} \, ||\boldsymbol{w}_1 - \boldsymbol{w}_2||_{1,r} & \text{if } 2d/(d+1) \leq r < \infty \, . \end{cases}$$

Proof.

$$\begin{aligned} j_1(\boldsymbol{v}_1, \boldsymbol{w}_2) - j_1(\boldsymbol{v}_1, \boldsymbol{w}_1) + j_1(\boldsymbol{v}_2, \boldsymbol{w}_1) - j_1(\boldsymbol{v}_2, \boldsymbol{w}_2) &\leq \kappa \int_S |\boldsymbol{v}_{1\boldsymbol{\tau}} - \boldsymbol{v}_{2\boldsymbol{\tau}}| \, |\boldsymbol{w}_{1\boldsymbol{\tau}} - \boldsymbol{w}_{2\boldsymbol{\tau}}| \\ &\leq \kappa\|\boldsymbol{v}_{1\boldsymbol{\tau}} - \boldsymbol{v}_{2\boldsymbol{\tau}}\|_{L^2(S)}\|\boldsymbol{w}_{1\boldsymbol{\tau}} - \boldsymbol{w}_{2\boldsymbol{\tau}}\|_{L^2(S)} \\ &\leq \kappa|||\boldsymbol{v}_1 - \boldsymbol{v}_2||| \, |||\boldsymbol{w}_1 - \boldsymbol{w}_2||| \end{aligned}$$

which is the desired result if $1 < r < 2d/(d+1)$, if not we use Lemma 2.1 .

About the existence and uniqueness of the variational solution of (2.6), we claim that

Theorem 2.1 (Existence and uniqueness)**.** *Let $\boldsymbol{f} \in \boldsymbol{V}'$, $g \in L^\infty(S)$, and $r \geq 2d/(d+1)$. Then Problem (2.6) has at least one solution $\boldsymbol{u} \in \boldsymbol{V}_{\rm div}$, moreover there is c such that*

$$||\boldsymbol{u}||_{1,r} \leq c\|\boldsymbol{f}\|_{\boldsymbol{V}'}^{1/(-1+r)}. \tag{2.7}$$

There is c depending on d, r and Ω such that if κ and $\boldsymbol{f}$ are defined such that

$$\begin{aligned} &c\kappa \leq \|\boldsymbol{f}\|_{\boldsymbol{V}'}^{\frac{r-2}{-1+r}} && \text{if } r > 2 \, , \\ &\text{or} \\ &\kappa\|\boldsymbol{f}\|_{\boldsymbol{V}'}^{\frac{2-r}{-1+r}} \leq c && \text{if } 2d/(d+1) \leq r < 2 \, , \end{aligned} \tag{2.8}$$

then the solution of (2.6) is unique.

Proof. The proof is done in several steps and we follow the method of proof in [31].

Step 1: Galerkin approximation. First, Since $\boldsymbol{V}_{\rm div}$ is separable, there are $\boldsymbol{\psi}_1, \boldsymbol{\psi}_2, ..., \boldsymbol{\psi}_n, ...$, elements of $\boldsymbol{V}_{\rm div}$, linear independent to each other such that

$$\bigcup_{n=1}^{\infty} \{\boldsymbol{\psi}_n\} \subset \boldsymbol{V}_{\rm div}, \qquad \overline{\{\boldsymbol{\psi}_1, \boldsymbol{\psi}_2, ..., \boldsymbol{\psi}_n, ...\}} = \boldsymbol{V}_{\rm div} \, .$$

Let $\boldsymbol{V}_{\rm div}^n = \{\boldsymbol{\psi}_1, \boldsymbol{\psi}_2, ..., \boldsymbol{\psi}_n\}$ be the space generated by the indicated vectors. For each $n \geq 1$ one considers the following approximate problem:

$$\begin{aligned} &\text{Find } \boldsymbol{u}_n \in \boldsymbol{V}_{\rm div}^n \text{ such that for all } i = 1, 2, 3, ..., n, \\ &\langle A\boldsymbol{u}_i, \boldsymbol{\psi}_i - \boldsymbol{u}_i\rangle + j_1(\boldsymbol{u}_i, \boldsymbol{\psi}_i) - j_1(\boldsymbol{u}_i, \boldsymbol{u}_i) \geq \langle \boldsymbol{f}, \boldsymbol{\psi}_i - \boldsymbol{u}_i\rangle \, . \end{aligned} \tag{2.9}$$

(2.9) is a nonlinear problem and in order to solve it, we implement a fixed point strategy. Thus for each $\boldsymbol{w} \in \boldsymbol{V}_{\rm div}^n$, we consider the problem:

$$\begin{aligned} &\text{Find } \boldsymbol{u}_n \in \boldsymbol{V}_{\rm div}^n \text{ such that for all } \boldsymbol{v} \in \boldsymbol{V}_{\rm div}^n, \\ &\langle A\boldsymbol{u}_n, \boldsymbol{v} - \boldsymbol{u}_n\rangle + j_1(\boldsymbol{w}, \boldsymbol{v}) - j_1(\boldsymbol{w}, \boldsymbol{u}_n) \geq \langle \boldsymbol{f}, \boldsymbol{v} - \boldsymbol{u}_n\rangle \, . \end{aligned} \tag{2.10}$$

For each $\boldsymbol{w} \in \boldsymbol{V}_{\rm div}$ the application $\boldsymbol{V}_{\rm div} \ni \boldsymbol{v} \longrightarrow j_1(\boldsymbol{w}, \boldsymbol{v})$ is continuous on $\boldsymbol{V}$ and having in mind Corollary 2.1, we can conclude at this step that (2.10) is uniquely solvable using the monotone operator theory (see [5],Theorem 2.1, p. 171).

Step 2: Fixed point method. We define the mapping

$$\begin{array}{rccl} \mathcal{F} & : \boldsymbol{V}^n_{\rm div} & \longrightarrow & \boldsymbol{V}^n_{\rm div} \\ & \boldsymbol{w} & \longrightarrow & \boldsymbol{u}_n\ , \quad \text{with } \boldsymbol{u}_n \text{ solution of (2.10).} \end{array} \tag{2.11}$$

We shall show that $\mathcal{F}$ has a fixed point using Leray-Schauder theorem.
First, we prove that for every $\boldsymbol{u}_n$ and $\lambda \in [0,1]$ satisfying $\lambda \mathcal{F}(\boldsymbol{u}_n) = \boldsymbol{u}_n$, we have

$$||\boldsymbol{u}_n||_{1,r} \leq c, \tag{2.12}$$

with c positive constant independent of n.
For $\lambda = 0$, $\boldsymbol{u}_n = \boldsymbol{0}$, hence (2.12) holds. Next for $\lambda > 0$, (2.10) implies that

$$\left\langle A\frac{\boldsymbol{u}_n}{\lambda}, \boldsymbol{v} - \frac{\boldsymbol{u}_n}{\lambda} \right\rangle + j_1(\boldsymbol{u}_n, \boldsymbol{v}) - j_1\left(\boldsymbol{u}_n, \frac{\boldsymbol{u}_n}{\lambda}\right) \geq \left\langle \boldsymbol{f}, \boldsymbol{v} - \frac{\boldsymbol{u}_n}{\lambda} \right\rangle . \tag{2.13}$$

We replace $\boldsymbol{v}$ successively in (2.13) by $\boldsymbol{0}$ and $\dfrac{2\boldsymbol{u}_n}{\lambda}$. Comparing the two inequalities, one obtains

$$\left\langle A\frac{\boldsymbol{u}_n}{\lambda}, \frac{\boldsymbol{u}_n}{\lambda} \right\rangle + j_1\left(\boldsymbol{u}_n, \frac{\boldsymbol{u}_n}{\lambda}\right) = \left\langle \boldsymbol{f}, \frac{\boldsymbol{u}_n}{\lambda} \right\rangle . \tag{2.14}$$

We then deduce (2.12) from (2.14), after application of Cauchy-Schwarz's inequality and Corollary 2.1.
Finally, we show that the map $\mathcal{F}$ is continuous with $W^{1,r}$-norm. Indeed let $\boldsymbol{w}^1, \boldsymbol{w}^2$ and $\boldsymbol{u}^1_n, \boldsymbol{u}^2_n$ such that $\mathcal{F}\boldsymbol{w}^1 = \boldsymbol{u}^1_n$, and $\mathcal{F}\boldsymbol{w}^2 = \boldsymbol{u}^2_n$. Then for all $\boldsymbol{v} \in \boldsymbol{V}^n_{\rm div}$ one has

$$\begin{aligned} &\langle A\boldsymbol{u}^1_n, \boldsymbol{v} - \boldsymbol{u}^1_n \rangle + j_1(\boldsymbol{w}^1, \boldsymbol{v}) - j_1(\boldsymbol{w}^1, \boldsymbol{u}^1_n) \geq \langle \boldsymbol{f}, \boldsymbol{v} - \boldsymbol{u}^1_n \rangle , \\ &\langle A\boldsymbol{u}^2_n, \boldsymbol{v} - \boldsymbol{u}^2_n \rangle + j_1(\boldsymbol{w}^2, \boldsymbol{v}) - j_1(\boldsymbol{w}^2, \boldsymbol{u}^2_n) \geq \langle \boldsymbol{f}, \boldsymbol{v} - \boldsymbol{u}^2_n \rangle . \end{aligned}$$

Taking $\boldsymbol{v} = \boldsymbol{u}^2_n$ in the first inequality, $\boldsymbol{v} = \boldsymbol{u}^1_n$ in the second inequality and adding the resulting inequalities gives

$$\langle A\boldsymbol{u}^1_n - A\boldsymbol{u}^2_n, \boldsymbol{u}^1_n - \boldsymbol{u}^2_n \rangle \leq j_1(\boldsymbol{w}^1, \boldsymbol{u}^2_n) - j_1(\boldsymbol{w}^1, \boldsymbol{u}^1_n) + j_1(\boldsymbol{w}^2, \boldsymbol{u}^1_n) - j_1(\boldsymbol{w}^2, \boldsymbol{u}^2_n) .$$

We readily obtain the continuity of $\mathcal{F}$ after application of Lemma 2.2, Lemma 2.1 and Lemma 2.3.
Thus we conclude that there exists a fixed point $\boldsymbol{u}_n$ of $\mathcal{F}$.

Step 3: A priori estimates and passage to the limit. We have;

$$\begin{aligned} &\text{for all } \boldsymbol{v} \in \boldsymbol{V}^n_{\rm div}, \\ &\langle A\boldsymbol{u}_n, \boldsymbol{v} - \boldsymbol{u}_n \rangle + j_1(\boldsymbol{u}_n, \boldsymbol{v}) - j_1(\boldsymbol{u}_n, \boldsymbol{u}_n) \geq \langle \boldsymbol{f}, \boldsymbol{v} - \boldsymbol{u}_n \rangle . \end{aligned} \tag{2.15}$$

Taking successively $\boldsymbol{v}$ equal $\boldsymbol{0}$ and $2\boldsymbol{u}_n$ in (2.15), and comparing the resulting inequalities, we obtain

$$\langle A\boldsymbol{u}_n, \boldsymbol{u}_n \rangle + j_1(\boldsymbol{u}_n, \boldsymbol{u}_n) = \langle \boldsymbol{f}, \boldsymbol{u}_n \rangle . \tag{2.16}$$

We then deduce thanks to Cauchy-Schwarz, Lemma 2.2, and Lemma 2.1 that there is c such that

$$||\boldsymbol{u}_n||_{1,r} \quad \leq \quad c\|\boldsymbol{f}\|^{1/(-1+r)}_{\boldsymbol{V}'}, \qquad \|A\boldsymbol{u}_n\|_{-1,r'} \leq c . \tag{2.17}$$

Hence there exists a subsequence denoted again $(\boldsymbol{u}_n)_n$ such that $\boldsymbol{u}_n \to \boldsymbol{u}$ weakly in $\boldsymbol{V}_{\rm div}$. The relation (2.15) is re-written as follows

$$\begin{aligned} &\text{for all } \boldsymbol{v} \in \boldsymbol{V}^n_{\rm div}, \\ &\langle A\boldsymbol{u}_n, \boldsymbol{u}_n \rangle + j_1(\boldsymbol{u}_n, \boldsymbol{u}_n) \leq \langle A\boldsymbol{u}_n, \boldsymbol{v} \rangle + j_1(\boldsymbol{u}_n, \boldsymbol{v}) - \langle \boldsymbol{f}, \boldsymbol{v} - \boldsymbol{u}_n \rangle . \end{aligned} \tag{2.18}$$

Let $\boldsymbol{v} \in \boldsymbol{V}^n_{\rm div}$, the application $\boldsymbol{w} \longrightarrow j_1(\boldsymbol{w}, \boldsymbol{v})$ is continuous and convex, together with the properties of A implies that

$$\begin{aligned} &\text{for all } \boldsymbol{v} \in \boldsymbol{V}^n_{\rm div}, \\ &\liminf_n \left[\langle A\boldsymbol{u}_n, \boldsymbol{u}_n \rangle + j_1(\boldsymbol{u}_n, \boldsymbol{u}_n)\right] \leq \langle A\boldsymbol{u}, \boldsymbol{v} \rangle + j_1(\boldsymbol{u}, \boldsymbol{v}) - \langle \boldsymbol{f}, \boldsymbol{v} - \boldsymbol{u} \rangle . \end{aligned} \tag{2.19}$$

Again from the properties of A and the fact that the application $\boldsymbol{w} \to j_1(\boldsymbol{w}, \boldsymbol{w})$ is continuous, we deduce that

$$\langle A\boldsymbol{u}, \boldsymbol{u}\rangle \leq \liminf_n \langle A\boldsymbol{u}_n, \boldsymbol{u}_n\rangle \quad , \qquad j_1(\boldsymbol{u}, \boldsymbol{u}) \leq \liminf_n j_1(\boldsymbol{u}_n, \boldsymbol{u}_n)\,.$$

We then conclude that there is at least $\boldsymbol{u} \in \boldsymbol{V}_{\rm div}$ such that

$$\begin{aligned} &\text{for all } \boldsymbol{v} \in \boldsymbol{V}_{\rm div}, \\ &\langle A\boldsymbol{u}, \boldsymbol{v}-\boldsymbol{u}\rangle + j_1(\boldsymbol{u}, \boldsymbol{v}) - j_1(\boldsymbol{u}, \boldsymbol{u}) \geq \langle \boldsymbol{f}, \boldsymbol{v}-\boldsymbol{u}\rangle\,. \end{aligned} \tag{2.20}$$

The inequality (2.7) is obtained from (2.20) by taking $\boldsymbol{v} = \boldsymbol{0}$, $\boldsymbol{v} = 2\boldsymbol{u}$ and utilization of Lemma 2.3. The unique solvability is obtained by assuming the existence of two solutions satisfying (2.20) and assuming (2.8).
It should be noted that the pressure in (2.6) is obtained by following [1, 5]. □

Remark 2.3. *We were not able to show the existence of solution when $1 < r < 2d/(d+1)$, the major hurdle being the derivation of the inequality*

$$\langle A\boldsymbol{u}^1 - A\boldsymbol{u}^2, \boldsymbol{u}^1 - \boldsymbol{u}^2\rangle \geq \beta |||\boldsymbol{u}^1 - \boldsymbol{u}^2|||^2 \ \textit{for all}\ \boldsymbol{u}^1, \boldsymbol{u}^2 \in \boldsymbol{V}\,,$$

which will ensure the continuity of the map $\mathcal{F}$ in $\boldsymbol{V}$.

The finite element approximation of (2.3), (2.4) is nonlinear problem, hence iterative solver is needed for the actual computation of solution. We note that the direct finite element formulation of (2.3), (2.4) has the following difficulties;

1. the inequality symbol,
2. the presence of the nonlinear term $|D(\boldsymbol{u})|^{r-2}$ when $r \neq 2$,
3. the non-differentiability of the term $|\boldsymbol{u}_{\boldsymbol{\tau}}|$.

For the problem at hand, it is noted that the presence of the inequality symbol is the consequence of the non-differentiable term $|\boldsymbol{u}_{\boldsymbol{\tau}}|$ on the boundary. Hence by regularizing the non-differentiable term with the help of the introduction of a small parameter, the variational problem (2.3), (2.4) is replaced by a regularized problem which is shown to be equivalent to a variational nonlinear equation. Thus iterative methods can be developed for computation of the numerical solution. It is worth noting that the regularization parameter may be taken in such a way that the approximate (regularized) model is as close as desired to the exact one (see [26, 27, 32, 33, 34]). In practice, the smaller the regularization parameter, the closer the approximate model to the exact one. In this work instead, we would like to solve the finite element approximation of (2.3), (2.4) using;

- the augmented Lagrangian algorithms based on the introduction of Lagrange multipliers depending on constraints,
- the interior point method .

It is important to mention that the augmented Lagrangian approach for the resolution of variational inequalities is based on the introduction of multiplier functions (called multipliers) and additional equation to remove the inequality symbol. The resulting system of equations is then solve with the help of Uzawa's type algorithm. The method is mathematically well grounded and has been used by many researchers in different context (see [26, 27, 32, 33]). The starting point of the methods we discuss in the next two sections is to observe that the problem (2.6) is equivalent to

$$\begin{aligned} &\text{Find } \boldsymbol{u} \in \boldsymbol{V}_{\rm div} \text{ such that for all } \boldsymbol{v} \in \boldsymbol{V}_{\rm div} \\ &J(\boldsymbol{u}) \leq J(\boldsymbol{v}) \ \text{ with} \\ &J(\boldsymbol{v}) = \frac{\nu_0}{r}\int_\Omega |D(\boldsymbol{v})|^r\,dx + \int_S g|\boldsymbol{v}_{\boldsymbol{\tau}}|d\sigma + \frac{\kappa}{2}\int_S |\boldsymbol{v}_{\boldsymbol{\tau}}|^2\,d\sigma - \langle \boldsymbol{f}, \boldsymbol{v}\rangle\ . \end{aligned} \tag{2.21}$$

It should be noted that the main difficulties for the numerical resolution of (2.21) are as follows; the poor differentiability of $|D(\boldsymbol{u})|^r$ for $1 < r < 2$, the presence of the non differentiable expression $|\boldsymbol{u}_{\boldsymbol{\tau}}|$.
The interior point strategy we discuss in this research is also based on the reformulation of the finite element approximation of (2.3), (2.4) as a minimization problem posed in a set with constraints. The constraints are then removed by introducing Lagrange multipliers functions (dual variables). The primal and dual variables are solved using saddle-point formalism, with the precision that the dual unknowns are computed using path-following algorithm.

3 Alternating direction method of multiplier 1

3.1 Augmented Lagrangian: Preliminaries

The main idea behind the augmented Lagrangian method which follows is to decouple the symmetry part of velocity gradient and the velocity; this is done by considering $D(\boldsymbol{u})$ as independent variable, say, $\mathbf{Z}$ and then by forcing the relation $\mathbf{Z} - D(\boldsymbol{u}) = 0$ by penalization and the use of a Lagrange multiplier. To put in practice the method, we introduce the space

$$\begin{aligned} \boldsymbol{Q} &= \{\mathbf{Z} = (z_{ij}),\ 1 \le i,j \le d\ ,\ z_{ij} = z_{ji}\ ,\ z_{ij} \in L^r(\Omega)\} = L^r_{\rm sym}(\Omega)^{d\times d}\,, \\ \boldsymbol{W} &= \{(\boldsymbol{v},\mathbf{Y})|\ \ \boldsymbol{v} \in \boldsymbol{V}_{\rm div},\ \mathbf{Y} \in \boldsymbol{Q}\ ,\ \ \mathbf{Y} - D(\boldsymbol{v}) = 0\}\ , \end{aligned}$$

and the functional

$$J(\boldsymbol{v},\mathbf{Y}) = \frac{\nu_0}{r}\int_\Omega |\mathbf{Y}|^r\,dx + \int_S g|\boldsymbol{v}_{\boldsymbol{\tau}}|d\sigma + \frac{\kappa}{2}\int_S |\boldsymbol{v}_{\boldsymbol{\tau}}|^2\,d\sigma - \langle \boldsymbol{f},\boldsymbol{v}\rangle\ .$$

It is then manifest that problem (2.21) is equivalent to

$$\begin{aligned} &\text{Find } (\boldsymbol{u},\mathbf{Z}) \in \boldsymbol{W} \text{ such that} \\ &J(\boldsymbol{u},\mathbf{Z}) \le J(\boldsymbol{v},\mathbf{Y}) \text{ for all } \boldsymbol{v},\mathbf{Y} \in \boldsymbol{W}\ . \end{aligned} \tag{3.1}$$

Next, with $\gamma > 0$, we define an augmented Lagrangian functional

$$\mathscr{L}_\gamma : \boldsymbol{V}_{\rm div} \times \boldsymbol{Q} \times L^{r'}_{\rm sym}(\Omega)^{d\times d} \longrightarrow \mathbb{R}\cup\{\infty\}$$

by

$$\mathscr{L}_\gamma(\boldsymbol{v},\mathbf{Y};\boldsymbol{\Lambda}) = J(\boldsymbol{v},\mathbf{Y}) + \int_\Omega \boldsymbol{\Lambda}\cdot(\mathbf{Y} - D(\boldsymbol{v}))dx + \frac{\gamma}{2}\int_\Omega |\mathbf{Y} - D(\boldsymbol{v})|^2 dx\ , \tag{3.2}$$

where $\boldsymbol{\Lambda}$ is the Lagrange multiplier, while γ is the inverse of the penalty parameter. Following [27], one notes that if $(\boldsymbol{u},\mathbf{Z};\boldsymbol{\Lambda})$ is a saddle point of $\mathscr{L}_\gamma$ over $\boldsymbol{V}_{\rm div}\times\boldsymbol{Q}\times L^\gamma_{\rm sym}(\Omega)^{d\times d}$, meaning that

$$\begin{cases} \text{for all } (\boldsymbol{v},\mathbf{Y};\boldsymbol{M}) \in \boldsymbol{V}_{\rm div}\times\boldsymbol{Q}\times L^{r'}_{\rm sym}(\Omega)^{d\times d} \\ \mathscr{L}_\gamma(\boldsymbol{u},\mathbf{Z};\boldsymbol{M}) \le \mathscr{L}_\gamma(\boldsymbol{u},\mathbf{Z};\boldsymbol{\Lambda}) \le \mathscr{L}_\gamma(\boldsymbol{v},\mathbf{Y};\boldsymbol{\Lambda})\,, \end{cases} \tag{3.3}$$

then the pair $(\boldsymbol{u},\mathbf{Z})$ is solution of the minimization problem (3.1), which implies, in turn that $\boldsymbol{u}$ is the solution of the minimization problem (2.21) with $\mathbf{Z} = D(\boldsymbol{u})$.

In order to characterize the saddle point of $\mathscr{L}_\gamma$, we recall the following fact

Lemma 3.1. *Let V a Reflexive Banach space.*
Let K be a nonempty closed convex subset of V.
Let J_0 be a convex functional Frechet or Gateaux differentiable on V.
Let J_1 be a proper l.s.c. convex functional.
Let $J = J_0 + J_1$ and assume that

$$\lim_{\|\boldsymbol{v}\|\to\infty} \frac{J(v)}{\|v\|} = \infty\,.$$

Then the minimization problem: Find $u \in K$ such that

$$J(u) \le J(v) \quad \textit{for all } v \in K,$$

has a solution $u \in K$ characterized by

$$\textit{for all}\ \ v \in K, \quad \langle J_0'(u), v-u\rangle + J_1(v) - J_1(u) \ge 0\,.$$

Remark 3.1. *We deduce from (3.3) and Lemma 3.1 that $(\boldsymbol{u},\boldsymbol{\lambda},\mathbf{Z})$ is characterized by the following relations: for all $(\boldsymbol{v},\boldsymbol{M}) \in \boldsymbol{V}_{\rm div}\times L^{r'}_{sym}(\Omega)^{d\times d}$*

$$\begin{cases} \gamma(D(\boldsymbol{u}), D(\boldsymbol{v}) - D(\boldsymbol{u}))_\Omega + \kappa(\boldsymbol{u}_{\boldsymbol{\tau}}, \boldsymbol{v}_{\boldsymbol{\tau}} - \boldsymbol{u}_{\boldsymbol{\tau}})_S + (g,|\boldsymbol{v}_{\boldsymbol{\tau}}|)_S - (g,|\boldsymbol{u}_{\boldsymbol{\tau}}|)_S \\ \ge (\boldsymbol{\Lambda}, D(\boldsymbol{v}) - D(\boldsymbol{u}))_\Omega + \gamma(\mathbf{Z}, D(\boldsymbol{v}) - D(\boldsymbol{u}))_\Omega + \langle \boldsymbol{f}, \boldsymbol{v}-\boldsymbol{u}\rangle\,, \\ \nu_0|\mathbf{Z}|^{r-2}\mathbf{Z} + \gamma\mathbf{Z} = \gamma D(\boldsymbol{u}) - \boldsymbol{\Lambda}\,, \\ (\mathbf{Z} - D(\boldsymbol{u}), \boldsymbol{M})_\Omega = 0\,. \end{cases} \tag{3.4}$$

3.2 Alternating direction method of multiplier

Applying an alternating direction method of multiplier (ADMM) to the saddle point problem (3.3) leads to the following iterative algorithm. Starting with $\mathbf{Z}^0$ and $\mathbf{\Lambda}^0$, we compute successively $\boldsymbol{u}^n$, $\mathbf{Z}^n$ and $\mathbf{\Lambda}^n$ as follows.

$$\begin{aligned} \boldsymbol{u}^{n+1} &= \arg\min_{\boldsymbol{v}\in\boldsymbol{V}_{\rm div}} \mathscr{L}_\gamma(\boldsymbol{v},\mathbf{Z}^n,\mathbf{\Lambda}^n) && (3.5)\\ \mathbf{Z}^{n+1} &= \arg\min_{\mathbf{Y}} \mathscr{L}_\gamma(\boldsymbol{u}^{n+1},\mathbf{Y},\mathbf{\Lambda}^n) && (3.6)\\ \mathbf{\Lambda}^{n+1} &= \mathbf{\Lambda}^n + \rho(\mathbf{Z}^{n+1} - D(\boldsymbol{u}^{n+1}))\,, && (3.7) \end{aligned}$$

with ρ a positive constant taken in such a way that the scheme (3.5)–(3.7) converges. Following [26, 27], the "safe" choice should be $\rho=\gamma$. Now owing to (3.4), the iterative process (3.5)–(3.7) is re-interpreted as follows: Given $(\boldsymbol{\lambda}^n,\mathbf{Z}^{n-1})$, compute $(\boldsymbol{u}^n,\mathbf{Z}^n,\boldsymbol{\lambda}^{n+1})$ such that

$$\begin{cases} \gamma(D(\boldsymbol{u}^n),D(\boldsymbol{v}-\boldsymbol{u}^n)\,) + \kappa(\boldsymbol{u}^n_{\boldsymbol{\tau}},\boldsymbol{v}_{\boldsymbol{\tau}}-\boldsymbol{u}^n_{\boldsymbol{\tau}})_S + (g,|\boldsymbol{v}_{\boldsymbol{\tau}}|)_S - (g,|\boldsymbol{u}^n_{\boldsymbol{\tau}}|)_S \\ \geq -(\mathbf{\Lambda}^n,D(\boldsymbol{v}-\boldsymbol{u}^n)\,) + \gamma(\mathbf{Z}^{n-1},D(\boldsymbol{v}-\boldsymbol{u}^n)\,) + \langle \boldsymbol{f},\boldsymbol{v}-\boldsymbol{u}^n\rangle\,, \\ \nu_0|\mathbf{Z}^n|^{r-2}\mathbf{Z}^n + \gamma\mathbf{Z}^n = \gamma D(\boldsymbol{u}^n) + \mathbf{\Lambda}^n\,, \\ \mathbf{\Lambda}^{n+1} = \mathbf{\Lambda}^n + \gamma(\mathbf{Z}^n - D(\boldsymbol{u}^n)), \end{cases} \tag{3.8}$$

Remark 3.2. *Note that the following algorithm may also be adopted*

$$\begin{aligned} \boldsymbol{u}^n &= \arg\min_{\boldsymbol{v}\in\boldsymbol{V}_{\rm div}} \mathscr{L}_\gamma(\boldsymbol{v},\mathbf{Z}^{n-1},\mathbf{\Lambda}^n) && (3.9)\\ \mathbf{\Lambda}^{n+1/2} &= \mathbf{\Lambda}^n + \gamma(\mathbf{Z}^{n-1} - D(\boldsymbol{u}^n)) && (3.10)\\ \mathbf{Z}^n &= \arg\min_{\mathbf{Y}\in\boldsymbol{Q}} \mathscr{L}_\gamma(\boldsymbol{u}^n,\mathbf{Y},\boldsymbol{\lambda}^{n+1/2}) && (3.11)\\ \mathbf{\Lambda}^{n+1} &= \mathbf{\Lambda}^{n+1/2} + \gamma(\mathbf{Z}^n - D(\boldsymbol{u}^n))\,. && (3.12) \end{aligned}$$

Decomposition-coordination methods (3.5)—(3.7) *and* (3.9)—(3.12) *can be interpreted as the numerical integration of associated evolution equation by well-known alternating-direction methods. In fact, see e.g. [32],* (3.5)—(3.7) *is equivalent to the classical Douglas-Rachford method while* (3.9)—(3.12) *is equivalent to the Peaceman-Rachford method.*

With regard to the feasibility of the algorithm (3.5)—(3.7) one introduces the following operators

$$\begin{aligned} \widetilde{a}(\boldsymbol{u}^n,\boldsymbol{v}) &= \gamma(D(\boldsymbol{u}^n),D(\boldsymbol{v})\,) + \kappa(\boldsymbol{u}^n_{\boldsymbol{\tau}},\boldsymbol{v}_{\boldsymbol{\tau}})_S\,, \\ \widetilde{j}(\boldsymbol{v}) &= (g,|\boldsymbol{v}_{\boldsymbol{\tau}}|)_S\,, \\ \widetilde{\ell}(\boldsymbol{v}) &= (-\mathbf{\Lambda}^n + \gamma\mathbf{Z}^{n-1},D(\boldsymbol{v})\,) + \langle \boldsymbol{f},\boldsymbol{v}\rangle\,. \end{aligned} \tag{3.13}$$

One readily check that; $\widetilde{a}(\cdot,\cdot)$ is linear, continuous, elliptic on $\boldsymbol{V}_{\rm div}$, $\widetilde{j}(\cdot)$ is l.s.c. convex and finally $\widetilde{\ell}(\cdot)$ is linear and continuous. Hence $\boldsymbol{u}^n$ is uniquely defined from (3.8). Next, the application $\boldsymbol{v}\longrightarrow\nu_0|\boldsymbol{v}|^{r-2}\boldsymbol{v}+\gamma\boldsymbol{v}$ is non-singular. Hence $\mathbf{Z}^n$ is well defined through the $\boldsymbol{z}$-equation of (3.8). The convergence analysis of the iterative scheme (3.8) is thoroughly discussed in [26, 27], hence it will not be re-repeated here. We claim that

Lemma 3.2. *The iterative scheme* (3.8) *is consistent with the variational problem* (3.4) *in the sense that if* $(\boldsymbol{u},\mathbf{Z})$ *is the solution of (3.4) and* $(\boldsymbol{\lambda}^0,\mathbf{Z}^0)=(\boldsymbol{\lambda},\mathbf{Z})$*, then for all* n*,* $(\boldsymbol{u}^n,\boldsymbol{\lambda}^n,\mathbf{Z}^n)=(\boldsymbol{u},\boldsymbol{\lambda},\mathbf{Z})$*.*

Proof. It is done by induction. Indeed, assume that for some n, $(\boldsymbol{u}^n,\boldsymbol{\lambda}^n,\mathbf{Z}^n)=(\boldsymbol{u},\boldsymbol{\lambda},\mathbf{Z})$. Then taking $\boldsymbol{v}=\boldsymbol{u}^{n+1}$ in (3.4) and $\boldsymbol{v}=\boldsymbol{u}$ in (3.8), and adding the resulting inequalities there holds

$$\widetilde{a}(\boldsymbol{u}^{n+1}-\boldsymbol{u},\boldsymbol{u}^{n+1}-\boldsymbol{u})\leq 0\,.$$

The coercivity of $a(\cdot,\cdot)$ implies that $\boldsymbol{u}^{n+1}=\boldsymbol{u}$.
Next, the second equation of (3.8) becomes

$$\boldsymbol{\lambda}^{n+1}=\boldsymbol{\lambda}+\rho(D(\boldsymbol{u})-\mathbf{Z})\,,$$

but from the third equation of (3.4), $\boldsymbol{\lambda} = D(\boldsymbol{u})$. Thus $\boldsymbol{\lambda}^{n+1} = \boldsymbol{\lambda}$. Finally from second equation of (3.4), and the third equation of (3.8), one has

$$\nu_0 \left\langle |\mathbf{Z}|^{r-2}\mathbf{Z} - |\mathbf{Z}^{n+1}|^{r-2}\mathbf{Z}^{n+1}, \mathbf{Z} - \mathbf{Z}^{n+1} \right\rangle + \gamma(\mathbf{Z} - \mathbf{Z}^{n+1}, \mathbf{Z} - \mathbf{Z}^{n+1}) = 0\,,$$

from which we deduce that $\mathbf{Z}^{n+1} = \mathbf{Z}$. We readily obtained from the fourth equation of (3.8) that $\boldsymbol{\lambda}^{n+1} = \boldsymbol{\lambda}$. □

3.3 Subproblem in z

The subproblem (3.6) can be reformulated as follows:

$$\begin{aligned} &\text{Find } \mathbf{Z} \in \boldsymbol{Q} \text{ such that for all } \mathbf{Y} \in \boldsymbol{Q} \\ &F(\mathbf{Z}) \leq F(\mathbf{Y})\,, \end{aligned} \tag{3.14}$$

with

$$F(\mathbf{Y}) = \frac{\nu_0}{r} \parallel \mathbf{Y} \parallel_{L^r}^r + \frac{\gamma}{2} \parallel \mathbf{Y} - D(\boldsymbol{u}^k) \parallel_{L^2}^2 + (\boldsymbol{\Lambda}^k, \mathbf{Y})_\Omega + \text{const}\,.$$

Since F is differentiable, its minimum is given by the nonlinear system of equations

$$\nu_0 |\mathbf{Z}|^{r-2}\mathbf{Z} + \gamma \mathbf{Z} = \gamma D(\boldsymbol{u}^k) - \boldsymbol{\Lambda}^k\ . \tag{3.15}$$

(3.15) is a nonlinear vectorial equation that can be solve in two steps as follows:
First take the length on both sides of the vectorial equation (3.15). This gives

$$\nu_0 |\mathbf{Z}|^{r-1} + \gamma |\mathbf{Z}| = |\gamma D(\boldsymbol{u}^k) - \boldsymbol{\Lambda}^k|\ . \tag{3.16}$$

We then solve (3.16) for $|\mathbf{Z}|$ using the method of Newton-Raphson or a fixed point approach. Secondly, we compute the components $\mathbf{Z}_{ij}$ as follows

$$\mathbf{Z}_{ij} = (\gamma D(\boldsymbol{u}^k) - \boldsymbol{\Lambda}^k)_{ij} \,/\, (\nu_0 |\mathbf{Z}|^{r-2} + \gamma) \quad \text{for all} \ \ i, j\,.$$

Note that with piecewise linear finite element, $D(\boldsymbol{u}^k)$ is constant on each triangle. Consequently, in view of (3.15), $\mathbf{Z}$ and $\boldsymbol{\Lambda}$ are constant on each triangle.

3.4 Subproblem in $\boldsymbol{u}$

If we set

$$G(\boldsymbol{v}) = \frac{\gamma}{2} \int_\Omega |D(\boldsymbol{v})|^2 dx - \int_\Omega (\gamma \mathbf{Z}^k + \boldsymbol{\Lambda}^k) : D(\boldsymbol{v})\, dx - \langle \boldsymbol{f}, \boldsymbol{v} \rangle, \tag{3.17}$$

the velocity subproblem reads

$$\begin{aligned} &\text{Find } \boldsymbol{u}^{k+1} \in \boldsymbol{V}_{div} \text{ such that,} \\ &G(\boldsymbol{u}^{k+1}) + j_1(\boldsymbol{u}^{k+1}, \boldsymbol{u}^{k+1}) \leq G(\boldsymbol{v}) + j_1(\boldsymbol{v}, \boldsymbol{v}) \quad \forall \boldsymbol{v} \in \boldsymbol{V}_{\text{div}}\ . \end{aligned} \tag{3.18}$$

Problem (3.18) is a linear Stokes problem with threshold slip boundary condition with γ as kinematic viscosity coefficient. Indeed, setting

$$\begin{aligned} a(\boldsymbol{u}, \boldsymbol{v}) &= \gamma (D(\boldsymbol{u}), D(\boldsymbol{v}))_\Omega, \\ b(\boldsymbol{v}, q) &= -(\text{div}\boldsymbol{v}, q)_\Omega \\ \ell(\boldsymbol{v}) &= \langle \boldsymbol{f}, \boldsymbol{v} \rangle + (\boldsymbol{\Lambda}^k + \gamma \mathbf{Z}^k, D(\boldsymbol{v}))_\Omega\,. \end{aligned}$$

we can show that (3.17) is equivalent to

$$\begin{aligned} &\text{Find } (\boldsymbol{u}, p) \text{ such that,} \\ &a(\boldsymbol{u}, \boldsymbol{v} - \boldsymbol{u}) + b(\boldsymbol{v} - \boldsymbol{u}, p) + j_1(\boldsymbol{u}, \boldsymbol{v}) - j_1(\boldsymbol{u}, \boldsymbol{u}) \geq \ell(\boldsymbol{v} - \boldsymbol{u}) \quad \forall \boldsymbol{v} \\ &b(\boldsymbol{v}, q) = 0 \quad \forall q. \end{aligned} \tag{3.19}$$

In [16], an alternating direction method of multiplier is proposed for solving (3.19). Setting $\boldsymbol{\phi} := \boldsymbol{u}_\tau$, we consider the constrained optimization problem: Find $(\boldsymbol{u}, \boldsymbol{\phi})$ such that

$$G(\boldsymbol{u}) + j_1(\boldsymbol{\phi}, \boldsymbol{\phi}) \ \leq \ G(\boldsymbol{v}) + j_1(\boldsymbol{\varphi}, \boldsymbol{\varphi}) \quad \forall (\boldsymbol{v}, \boldsymbol{\varphi}) \tag{3.20}$$

$$\boldsymbol{\phi} - \boldsymbol{u}_\tau \ = \ 0 \ \text{ on } S. \tag{3.21}$$

With (3.20)-(3.21), we associate the augmented Lagrangian functional

$$\mathscr{L}_{\gamma_2}(\boldsymbol{v},\boldsymbol{\phi},\boldsymbol{\lambda}) = G(\boldsymbol{v}) + j_1(\boldsymbol{\phi},\boldsymbol{\phi}) + \int_S (\boldsymbol{\phi}-\boldsymbol{v}_\tau)\cdot\boldsymbol{\lambda}\, d\sigma + \frac{\gamma_2}{2}\int_S |\boldsymbol{\phi}-\boldsymbol{v}_\tau|^2 d\sigma, \tag{3.22}$$

where $\gamma_2 > 0$ is the inverse of the penalty parameter. Applying an ADMM method to (4.4) we get Algorithm 1 (see [16] for details). We iterate until the relative error on $(\boldsymbol{u}^n, \boldsymbol{\phi}^n)$ becomes "sufficiently" small.

Algorithm 1 ADMM for the Stokes problem with stick/slip boundary condition (3.19)

Iteration $n = 0$**.** $\gamma_2 > 0$, $\boldsymbol{\phi}^0$ and $\boldsymbol{\lambda}^0$ are given.

Iteration $n \geq 0$**.** Compute successively $\boldsymbol{u}^{n+1}$, $\boldsymbol{\phi}^{n+1}$ and $\boldsymbol{\lambda}^{n+1}$ as follows.

1. Find $(\boldsymbol{u}^{n+1}, p^{n+1}) \in \boldsymbol{V} \times L^2_0(\Omega)$ such that for all $(\boldsymbol{v}, q) \in \boldsymbol{V} \times L^2(\Omega)$,

$$\begin{aligned} a(\boldsymbol{u}^{n+1},\boldsymbol{v}) + \gamma_2(\boldsymbol{u}^{n+1}_\tau,\boldsymbol{v}_\tau)_S + b(\boldsymbol{v},p^{n+1}) &= \ell(\boldsymbol{v})\ , \\ b(\boldsymbol{u}^{n+1},q) &= 0\,. \end{aligned}$$

2. Setting $\rho^n = |\gamma_2\boldsymbol{u}^{n+1}_\tau - \boldsymbol{\lambda}^n|$ and $(\rho^n - g)^+ = \max(0, \rho^n - g)$

$$\boldsymbol{\phi}^{n+1} = \frac{(\rho^n - g)^+}{(\gamma_2 + k)\rho^n}\left(\gamma_2\boldsymbol{u}^{n+1}_\tau - \boldsymbol{\lambda}^n\right)$$

3. Lagrange multiplier:

$$\boldsymbol{\lambda}^{n+1} = \boldsymbol{\lambda}^n + \gamma_2(\boldsymbol{\phi}^{n+1} - \boldsymbol{u}^{n+1}_\tau)$$

An efficient solution method is proposed in Section 5 based on the path-following variant of the interior point method [28].

3.5 Algorithm

Gathering the results of the previous subsections, we obtain the alternating direction method of multiplier outlined in Algorithm 2. As for Algorithm 1, we iterate until the relative error on $(\boldsymbol{u}^k, p^k, \mathbf{Z}^k)$ becomes "sufficiently" small.

Algorithm 2 First ADMM for the nonlinear Stokes problem with stick/slip boundary condition

Iteration $k = 0$**.** $\gamma > 0$, $\gamma_2 > 0$, $\mathbf{Z}^0$ and $\boldsymbol{\Lambda}^0$ are given.

Iteration $k \geq 0$**.** Compute successively $(\boldsymbol{u}^{k+1}, p^{k+1})$, $\mathbf{Z}^{k+1}$ and $\boldsymbol{\Lambda}^{k+1}$ as follows.

1. Solve (3.19) for $(\boldsymbol{u}^{k+1}, p^{k+1})$ using Algorithm 1
2. Compute $q \geq 0$ such that

$$\nu_0 q^{r-1} + \gamma q = |\gamma D(\boldsymbol{u}^k) - \boldsymbol{\Lambda}^k|.$$

and

$$\mathbf{Z}^{k+1}_{ij} = (\gamma D(\boldsymbol{u}^k) - \boldsymbol{\Lambda}^k)_{ij} \,/\, (\nu_0 q^{r-2} + \gamma)\,.$$

3. Update the multiplier

$$\boldsymbol{\Lambda}^{k+1} = \boldsymbol{\Lambda}^k + \gamma(\mathbf{Z}^{k+1} - D(\boldsymbol{u}^{k+1})).$$

4 Alternating direction method of multiplier 2

A one-loop ADMM algorithm can be derived for non linear Stokes problem by introducing the auxiliary unknowns $\mathbf{Z} := D(\boldsymbol{u})$ and $\boldsymbol{\phi} := \boldsymbol{u}_\tau$ at the same time such that, instead of (3.1), we consider

Find $(\boldsymbol{u}, \mathbf{Z}, \boldsymbol{\phi})$ such that

$$J(\boldsymbol{u}, \mathbf{Z}) + j_1(\boldsymbol{\phi}, \boldsymbol{\phi}) \leq J(\boldsymbol{v}, \mathbf{Y}) + j_1(\boldsymbol{\varphi}, \boldsymbol{\varphi}) \quad \forall (\boldsymbol{v}, \mathbf{Y}, \varphi) \tag{4.1}$$

$$\mathbf{Z} - D(\boldsymbol{u}) = 0, \quad \text{in } \Omega \tag{4.2}$$

$$\boldsymbol{\phi} - \boldsymbol{u}_\tau = 0, \quad \text{on } S. \tag{4.3}$$

The corresponding augmented Lagrangian functional is then

$$\begin{aligned} \mathscr{L}_\gamma(\boldsymbol{v}, \mathbf{Y}, \boldsymbol{\phi}, \boldsymbol{\Lambda}, \lambda) &= J(\boldsymbol{v}, \mathbf{Y}) + j_1(\boldsymbol{\phi}, \boldsymbol{\phi}) + \int_\Omega (\mathbf{Y} - D(\boldsymbol{v})) : \boldsymbol{\Lambda}\, dx + \int_S (\boldsymbol{\phi} - \boldsymbol{v}_\tau) \cdot \boldsymbol{\lambda}\, d\sigma \\ &\quad + \frac{\gamma}{2} \int_\Omega |\mathbf{Y} - D(\boldsymbol{v})|^2 dx + \frac{\gamma}{2} \int_S |\boldsymbol{\phi} - \boldsymbol{v}_\tau|^2 d\sigma\,. \end{aligned} \tag{4.4}$$

Applying an alternating direction method of multiplier to (4.4), we get the following iterative process

$$\boldsymbol{u}^{k+1} = \arg \min_{\boldsymbol{v} \in \boldsymbol{V}_{\text{div}}} \mathscr{L}_\gamma(\boldsymbol{v}, \mathbf{Z}^k, \boldsymbol{\phi}^k, \boldsymbol{\Lambda}^k, \boldsymbol{\lambda}^k) \tag{4.5}$$

$$(\mathbf{Z}^{k+1}, \boldsymbol{\phi}^{k+1}) = \arg \min_{(\mathbf{Y}, \boldsymbol{\varphi})} \mathscr{L}_\gamma(\boldsymbol{u}^{k+1}, \mathbf{Y}, \boldsymbol{\varphi}, \boldsymbol{\Lambda}^k, \boldsymbol{\lambda}^k) \tag{4.6}$$

$$\boldsymbol{\Lambda}^{k+1} = \boldsymbol{\Lambda}^k + \gamma(\mathbf{Z}^{k+1} - D(\boldsymbol{u}^{k+1})) \tag{4.7}$$

$$\boldsymbol{\lambda}^{k+1} = \boldsymbol{\lambda}^k + \gamma(\boldsymbol{\phi}^{k+1} - \boldsymbol{u}_\tau^{k+1}). \tag{4.8}$$

The velocity subproblem (4.5) reads

Find $(\boldsymbol{u}^{k+1}, p^{k+1})$ such that

$$\gamma(D(\boldsymbol{u}^{k+1}), D(\boldsymbol{v}))_\Omega + \gamma(\boldsymbol{u}^{k+1}, \boldsymbol{v})_S + b(\boldsymbol{v}, p) = \ell^k(\boldsymbol{v}), \quad \forall \boldsymbol{v} \tag{4.9}$$

$$b(\boldsymbol{u}, q) = 0 \quad \forall q \tag{4.10}$$

where we have set

$$\ell^k(\boldsymbol{v}) = \langle \boldsymbol{f}, \boldsymbol{v} \rangle + (\boldsymbol{\Lambda}^k + \gamma \mathbf{Z}^k, D(\boldsymbol{v}))_\Omega + (\boldsymbol{\lambda}^k + \gamma \boldsymbol{\phi}^k, \boldsymbol{v}_\tau)_S.$$

Problem (4.9)-(4.10) is a linear Stokes problem with an additional mass term on the frictional boundary S.

In (4.6), subproblems in $\mathbf{Z}$ and $\boldsymbol{\phi}$ are uncoupled. Furthermore, the subproblem in $\mathbf{Z}$ is the same as in Section 3.3 while the subproblem in $\boldsymbol{\phi}$ is the same as in Section 3.4. The ADMM algorithm, using the constrained minimization (4.1)-(4.3), is outlined in Algorithm 3.

Remark 4.1. *It is worth noting in algorithm 2 that we have separated $\boldsymbol{u}$ from $D(\boldsymbol{u})$ by introducing a Lagrange multiplier, while algorithm 3 makes use of two Lagrange multipliers in order to separate $\boldsymbol{u}$, $D(\boldsymbol{u})$ and $\boldsymbol{u}_{\boldsymbol{\tau}}$.*
Even though the iterative scheme (4.5)—(4.8) uses two Lagrange multipliers, the way to study its convergence will be the same as the convergence analysis of the scheme (3.8) discussed in [26, 27].

Algorithm 3 Second ADMM for the nonlinear Stokes problem with stick/slip boundary condition

Iteration $n = 0$**.** $\gamma > 0$, $\mathbf{Z}^0$, $\boldsymbol{\phi}^0$, $\boldsymbol{\Lambda}^0$ and $\boldsymbol{\lambda}^0$ are given.

Iteration $n \geq 0$**.** Compute successively $\boldsymbol{u}^{n+1}$, $\mathbf{Z}^{n+1}$, $\boldsymbol{\phi}^{n+1}$, $\boldsymbol{\Lambda}^{n+1}$ and $\boldsymbol{\lambda}^{n+1}$ as follows.

1. Find $(\boldsymbol{u}^{n+1}, p^{n+1}) \in \boldsymbol{V} \times L^2_0(\Omega)$ such that

$$\begin{aligned} \gamma a(\boldsymbol{u}^{n+1}, \boldsymbol{v}) + \gamma(\boldsymbol{u}^{n+1}, \boldsymbol{v})_S + b(\boldsymbol{v}, p) &= \ell^n(\boldsymbol{v}), \quad \forall \boldsymbol{v} \in \boldsymbol{V} \\ b(\boldsymbol{u}, q) &= 0, \quad \forall q \in L^2(\Omega). \end{aligned}$$

2. Setting $\rho^n = |\gamma \boldsymbol{u}_\tau^{n+1} - \boldsymbol{\lambda}^n|$ and $(\rho^n - g)^+ = \max(0, \rho^n - g)$

$$\boldsymbol{\phi}^{n+1} = \frac{(\rho^n - g)^+}{(\gamma + \kappa)\rho^n} \left(\gamma \boldsymbol{u}_\tau^{n+1} - \boldsymbol{\lambda}^n\right)$$

3. Compute $q \geq 0$ such that

$$\nu_0 q^{r-1} + \gamma q = |\gamma D(\boldsymbol{u}^n) - \boldsymbol{\Lambda}^n|,$$

and

$$\mathbf{Z}_{ij}^{n+1} = (\gamma D(\boldsymbol{u}^n) - \boldsymbol{\Lambda}^n)_{ij} \,/\, (\nu_0 q^{r-2} + \gamma)\,.$$

4. Update the Lagrange multipliers

$$\begin{aligned} \boldsymbol{\Lambda}^{n+1} &= \boldsymbol{\Lambda}^n + \gamma(\mathbf{Z}^{n+1} - D(\boldsymbol{u}^{n+1})). \\ \boldsymbol{\lambda}^{n+1} &= \boldsymbol{\lambda}^n + \gamma(\boldsymbol{\phi}^{n+1} - \boldsymbol{u}_\tau^{n+1}) \end{aligned}$$

5 Numerical solution of subproblem in u with an interior point method

We introduce the algebraic problem arising from the mixed finite element approximation of (3.18) based on P1-bubble/P1 finite element. Then, we recall some main ideas of the path-following variant of the interior point method that is used for his resolution. In advance, we assume the Neumann boundary condition on Γ_N so that $\partial\Omega = \overline{\Gamma_D} \cup \overline{S} \cup \overline{\Gamma}_N$.

5.1 Algebraic representation

The finite element approximation of (3.18) leads to the algebraic problem:

Find $(\mathbf{u}, \mathbf{p}) \in \mathbb{R}^{n_u} \times \mathbb{R}^{n_p}$ such that $\forall \mathbf{v} \in \mathbb{R}^{n_u}$ and $\forall \mathbf{q} \in \mathbb{R}^{n_p}$

$$\begin{aligned} \mathbf{u}^\top \mathbf{A}(\mathbf{v}-\mathbf{u}) + (\mathbf{v}-\mathbf{u})^\top \mathbf{B}^\top \mathbf{p} + \mathbf{g}^\top(|\mathbf{T}\mathbf{v}| - |\mathbf{T}\mathbf{u}|) &\geq \mathbf{l}^\top(\mathbf{v}-\mathbf{u}), && (5.1)\\ \mathbf{q}^\top \mathbf{B}\mathbf{u} &= 0, && (5.2)\\ \mathbf{N}\mathbf{u} &= \mathbf{0}, && (5.3) \end{aligned}$$

where $\mathbf{u}$, $\mathbf{p}$ is the vector of the nodal values of the velocity $\boldsymbol{u}$ and the pressure p, respectively, $\mathbf{A} \in \mathbb{R}^{n_u \times n_u}$ is a symmetric and positive definite stiffness matrix, $\mathbf{B} \in \mathbb{R}^{n_p \times n_u}$ is the full row-rank divergence matrix, $\mathbf{T}, \mathbf{N} \in \mathbb{R}^{n_c \times n_u}$ are full row-rank matrices composed by the normal, tangential vectors lying on the slip boundary S, respectively, and $\mathbf{l} \in \mathbb{R}^{n_u}$ is the load vector including the Neumann boundary condition on Γ_N. For $\mathbf{u} \in \mathbb{R}^{n_u}$, $\mathbf{N}\mathbf{u}$ is the vector of the normal coordinates of $\mathbf{u}$ at the slip nodes, and $\mathbf{T}\mathbf{u}$ is the tangential coordinates of $\mathbf{u}$ at the contact nodes. The slip boundary condition represented by the functional J_1 from (2.5) can be divided into two parts:

$$J_1(\boldsymbol{v}, \boldsymbol{v}) = (\kappa|\boldsymbol{v}_{\boldsymbol{\tau}}|, |\boldsymbol{v}_{\boldsymbol{\tau}}|)_S + (g, |\boldsymbol{v}_{\boldsymbol{\tau}}|)_S.$$

As the first part is the quadratic form, it is included in the stiffness matrix $\mathbf{A}$. The second part is sub linear. It leads to the sub linear term in (5.1), in which $\mathbf{g} \in \mathbb{R}^{n_c}_+$ is the vector of the nodal slip bound values on S. Further $|\mathbf{x}| = (|x_1|, \ldots, |x_{n_c}|)^\top$ for $\mathbf{x} \in \mathbb{R}^{n_c}$; n_p is the total number of the nodes of a used triangulation contained in $\overline{\Omega}$, n_c is the number of the nodes lying on $S \setminus \Gamma$, and n_u is the dimension of the solution component representing the velocity $\mathbf{u}$.

It is easy to show that the algebraic problem (5.1)- (5.3) is equivalent to the following minimization problem:

$$\begin{aligned} &\text{Find } \mathbf{u} \in \mathbb{V} \text{ such that } \mathcal{J}(\mathbf{u}) \leq \mathcal{J}(\mathbf{v}) \text{ for all } \mathbf{v} \in \mathbb{V}\,,\\ &\text{with } \mathcal{J}(\mathbf{v}) = \frac{1}{2}\mathbf{v}^\top \mathbf{A}\mathbf{v} - \mathbf{v}^\top \mathbf{l} + \mathbf{g}^\top |\mathbf{T}\mathbf{v}|\,, \qquad (5.4)\\ &\text{and } \mathbb{V} = \{\mathbf{v} \in \mathbb{R}^{n_u} :\ \mathbf{N}\mathbf{v} = \mathbf{0},\ \mathbf{B}\mathbf{v} = \mathbf{0}\}\,. \end{aligned}$$

To release the discrete impermeability condition $\mathbf{N}\mathbf{v} = \mathbf{0}$ and to regularize the last non-differentiable slip term in $\mathcal{J}$, we introduce two algebraic Lagrange multipliers $\boldsymbol{\lambda}_n$ and $\boldsymbol{\lambda}_t$, respectively, and define the Lagrangian $\mathcal{L} : \mathbb{R}^{n_u} \times \Sigma \mapsto \mathbb{R}$ by

$$\mathcal{L}(\mathbf{v}, \boldsymbol{\lambda}) = \frac{1}{2}\mathbf{v}^\top \mathbf{A}\mathbf{v} - \mathbf{v}^\top \mathbf{l} + \boldsymbol{\lambda}^\top \mathbf{C}\mathbf{v},$$

where

$$\begin{aligned} &\Sigma = \{\boldsymbol{\lambda}_t \in \mathbb{R}^{n_c} :\ |\boldsymbol{\lambda}_t| \leq \mathbf{g}\} \times \mathbb{R}^{n_c + n_p}\,,\\ &\boldsymbol{\lambda} = (\boldsymbol{\lambda}_t^\top, \boldsymbol{\lambda}_n^\top, \mathbf{p}^\top)^\top \in \Sigma\,,\\ &\mathbf{C} = (\mathbf{T}^\top, \mathbf{N}^\top, \mathbf{B}^\top)^\top\,. \end{aligned}$$

The minimization problem (5.4) is equivalent to the following *saddle-point* formulation:

$$\begin{aligned} &\text{Find } (\mathbf{u}, \widetilde{\lambda}) \in \mathbb{R}^{n_u} \times \Sigma \text{ such that}\,,\\ &\mathcal{L}(\mathbf{u}, \boldsymbol{\lambda}) \leq \mathcal{L}(\mathbf{u}, \widetilde{\boldsymbol{\lambda}}) \leq \mathcal{L}(\mathbf{v}, \widetilde{\boldsymbol{\lambda}}) \quad \forall (\mathbf{v}, \boldsymbol{\lambda}) \in \mathbb{R}^{n_u} \times \Sigma\,. \end{aligned} \qquad (5.5)$$

From the second inequality in the problem (5.5) we see that

$$\mathbf{u} = \mathbf{A}^{-1}(\mathbf{l} - \mathbf{C}^\top \widetilde{\boldsymbol{\lambda}})\,. \qquad (5.6)$$

Inserting into the first inequality in the problem (5.5), we get the dual problem in terms of $\boldsymbol{m}\lambda$ only:

$$\textit{Find } \widetilde{\boldsymbol{\lambda}} \in \Lambda \textit{ such that } \mathcal{S}(\widetilde{\boldsymbol{\lambda}}) \leq \mathcal{S}(\boldsymbol{\lambda}) \quad \forall \boldsymbol{\lambda} \in \Sigma \tag{5.7}$$

with $\mathcal{S}(\boldsymbol{\lambda}) = \frac{1}{2}\boldsymbol{\lambda}^\top \mathbf{F}\boldsymbol{\lambda} - \boldsymbol{\lambda}^\top \mathbf{d}$, where $\mathbf{F} = \mathbf{C}\mathbf{A}^{-1}\mathbf{C}^\top$ is symmetric, positive definite, and $\mathbf{d} = \mathbf{C}\mathbf{A}^{-1}\mathbf{l}$. The dual formulation (5.7) is the minimization of the strictly quadratic function $\mathcal{S}$ subject to a small number (n_c) of constrained unknowns versus a large number ($n_c + n_p = n_c + \mathcal{O}(n_c^2)$) of the unconstrained ones. The optimization algorithm appropriate for problems with this structure is described below.

5.2 Path-following algorithm

We present the path-following variant of the interior point method ([35]) developed in [28]. Originally this algorithm was used for solving contact problems with friction in solid mechanics. Its performance was comparable with other frequently used algorithms based on the active set strategy or on the semi-smooth Newton method. Unlike contact problems, where the dual variables (discrete normal and tangential contact stresses) are located only on a contact part of the boundary, the situation in problems studied in this paper is quite different. In addition to the "boundary" dual variables, this time the pressure appears, i.e., the number of primal variables (the discrete velocity field) is comparable with the number of the dual variables (discrete shear and normal stress on the slip boundary + discrete pressure in the whole domain). Consequently, the elimination of the velocity field still leads to a large scale problem. The interior point algorithm was tested and compared with the ones mentioned above using several academic examples. Computational experiments proved its superiority over the active set strategy and semi-smooth methods: the method requires a number of iterations that increases very moderately with the increasing number of degree of freedoms, i.e., it scales also for our kind of problems (see [36]). There is yet another benefit of this method, namely the algorithm can be easily modified for the parallel implementation, which is based on the TFETI (Finite Element Tearing and Interconnecting) domain decomposition technique as shown in [38]. Only computational aspects of this method are mentioned in what follows, while the convergence analysis can be found in [28].

The Lagrangian to the dual problem (5.7) is given by

$$L(\boldsymbol{\lambda}, \boldsymbol{\mu}) = \mathcal{S}(\boldsymbol{\lambda}) + \boldsymbol{\mu}_1^\top(-\boldsymbol{\lambda}_t - \mathbf{g}) + \boldsymbol{\mu}_2^\top(\boldsymbol{\lambda}_t - \mathbf{g}),$$

where $\boldsymbol{\mu} = (\boldsymbol{\mu}_1^\top, \boldsymbol{\mu}_2^\top)^\top \in \mathbb{R}^{2n_c}$ is the Lagrange multiplier releasing two sided constraint appearing in the feasible set Σ. Let us define the new variable $\mathbf{z} := -\nabla_{\boldsymbol{\mu}} L(\boldsymbol{\lambda}, \boldsymbol{\mu})$ and the function $\mathbf{G} : \mathbb{R}^{6n_c+n_p} \mapsto \mathbb{R}^{6n_c+n_p}$ by

$$\mathbf{G}(\mathbf{w}) := (\nabla_\lambda L(\boldsymbol{\lambda}, \boldsymbol{\mu})^\top, (\nabla_\mu L(\boldsymbol{\lambda}, \boldsymbol{\mu}) + \mathbf{z})^\top, \mathbf{e}^\top \mathbf{M}\mathbf{Z})^\top,$$

where $\mathbf{w} = (\boldsymbol{\lambda}^\top, \boldsymbol{\mu}^\top, \mathbf{z}^\top)^\top \in \mathbb{R}^{6n_c+n_p}$, $\mathbf{M} = diag(\boldsymbol{\mu})$, $\mathbf{Z} = diag(\mathbf{z})$, and $\mathbf{e} \in \mathbb{R}^{2n_c}$ is the vector with all components equal to one. The solution $\widetilde{\boldsymbol{\lambda}}$ to (5.7) is the first component of the vector $\widetilde{\mathbf{w}} = (\widetilde{\boldsymbol{\lambda}}^\top, \widetilde{\boldsymbol{\mu}}^\top, \widetilde{\mathbf{z}}^\top)^\top$ which satisfies

$$\mathbf{G}(\mathbf{w}) = \mathbf{0}, \ \boldsymbol{\mu} \geq \mathbf{0}, \ \mathbf{z} \geq \mathbf{0}, \tag{5.8}$$

since (5.8) is equivalent to the respective Karush-Khun-Tucker conditions. The inequalities in (5.8) and later should be understood componentwise. To derive the path-following algorithm, we replace (5.8) by the following perturbed problem:

$$\mathbf{G}(\mathbf{w}) = (\mathbf{0}^\top, \mathbf{0}^\top, \tau\mathbf{e}^\top)^\top, \ \boldsymbol{\mu} > 0, \ \mathbf{z} > \mathbf{0}, \tag{5.9}$$

where $\tau \in \mathbb{R}_+$. Solutions $\mathbf{w}^\tau$ to (5.9) define a curve $\mathcal{C}(\tau)$ in $\mathbb{R}^{6n_c+n_p}$ called the *central path* that approaches $\widetilde{\mathbf{w}}$ when τ tends to zero. Our algorithm combines the damped Newton method for solving the equation in (5.9) with an appropriate change of τ, which guarantees that the iterations belong to a neighborhood of $\mathcal{C}(\tau)$ defined by, setting $\mathbf{w} = (\boldsymbol{\lambda}^\top, \boldsymbol{\mu}^\top, \mathbf{z}^\top)^\top$

$$\begin{aligned} \mathcal{N}(c_1, c_2) \quad = \quad & \big\{\mathbf{w} \in \mathbb{R}^{6n_c+n_p} : \mu_i z_i \geq c_1\vartheta, \ i = 1, \ldots, 2n_c, \ \boldsymbol{\mu} \geq \mathbf{0}, \ \mathbf{z} \geq \mathbf{0}\ , \\ & \|\nabla_\lambda L(\boldsymbol{\lambda}, \boldsymbol{\mu})\| \leq c_2\vartheta, \ \|\nabla_\mu L(\boldsymbol{\lambda}, \boldsymbol{\mu}) + \mathbf{z}\| \leq c_2\vartheta\big\}\ , \end{aligned}$$

where $c_1 \in (0, 1]$, $c_2 \geq 0$, and $\vartheta := \vartheta(\mathbf{w}) = \boldsymbol{\mu}^\top\mathbf{z}/(2n_c)$. In the k-th iteration, we modify $\tau := \tau^{(k)}$ by the product of $\vartheta^{(k)} = \vartheta(\mathbf{w}^{(k)})$ with the centering parameter $c^{(k)}$ chosen as in [37].

To get the monotonically decreasing sequence $\{\vartheta^{(k)}\}$, the algorithm uses also the *Armijo-type condition* (5.11). By $\mathbf{J}(\mathbf{w})$ in (5.10), we denote the Jacobi matrix of $\mathbf{G}$ at $\mathbf{w}$. The bounds on the parameters mentioned in the initialization section follow from the convergence analysis presented in [28].

Algorithm 4 Path-following interior point algorithm for (5.1),(5.2),(5.3)

Given $c_1 \in (0,1]$, $c_2 \geq 1$, $0 < c_{\min} \leq c_{\max} \leq 1/2$, $\omega \in (0,1)$, and $\varepsilon \geq 0$. Let $\mathbf{w}^{(0)} \in \mathcal{N}(c_1, c_2)$ and set $k := 0$.

(i). Choose $c^{(k)} \in [c_{\min}, c_{\max}]$.

(ii). Solve

$$\mathbf{J}(\mathbf{w}^{(k)})\Delta\mathbf{w}^{(k+1)} \;=\; -\mathbf{G}(\mathbf{w}^{(k)}) + (\mathbf{0}^\top, \mathbf{0}^\top, c^{(k)}\vartheta^{(k)}\mathbf{e}^\top)^\top. \tag{5.10}$$

(iii). Set $\mathbf{w}^{(k+1)} = \mathbf{w}^{(k)} + \alpha^{(k)}\Delta\mathbf{w}^{(k+1)}$ with the largest $\alpha^{(k)} \in (0,1]$ satisfying $\mathbf{w}^{(k+1)} \in \mathcal{N}(c_1, c_2)$ and

$$\vartheta^{(k+1)} \leq (1 - \alpha^{(k)}\omega(1 - c^{(k)}))\vartheta^{(k)}. \tag{5.11}$$

(iv). Return $\widetilde{\mathbf{w}} = \mathbf{w}^{(k+1)}$, if $err^{(k)} := \|\mathbf{w}^{(k+1)} - \mathbf{w}^{(k)}\|/\|\mathbf{w}^{(k+1)}\| \leq \varepsilon$, else set $k := k + 1$ and go to step (i).

The computational efficiency depends on a way how the inner linear systems in (5.10) are solved. Although the Jacobi matrix is non-symmetric, indefinite with the following block structure:

$$\mathbf{J}(\mathbf{w}^{(k)}) = \begin{pmatrix} \mathbf{F} & \begin{pmatrix} -\mathbf{I} & \mathbf{I} \\ \mathbf{0} & \mathbf{0} \end{pmatrix} & \mathbf{0} \\ \begin{pmatrix} -\mathbf{I} & \mathbf{0} \\ \mathbf{I} & \mathbf{0} \end{pmatrix} & \mathbf{0} & \mathbf{I} \\ \mathbf{0} & \mathbf{Z} & \mathbf{M} \end{pmatrix},$$

the methods for symmetric, positive definite linear systems may be used. Eliminating the 2nd and 3rd unknown in $\Delta\mathbf{w}^{(k+1)}$, we arrive at the reduced linear system for $\Delta\boldsymbol{\lambda}^{(k+1)}$ with the Schur complement $\mathbf{J}_{SC} = \mathbf{F} + \mathbf{M}_1\mathbf{Z}_1^{-1} + \mathbf{M}_2\mathbf{Z}_2^{-1}$, where $\mathbf{Z} = diag(\mathbf{Z}_1, \mathbf{Z}_2)$ and $\mathbf{M} = diag(\mathbf{M}_1, \mathbf{M}_2)$. As $\boldsymbol{\mu}^{(k)} > \mathbf{0}$, $\mathbf{z}^{(k)} > \mathbf{0}$, the matrix $\mathbf{J}_{SC}$ is symmetric, positive definite and the reduced linear system can be solved by the conjugate gradient method. However, $\mathbf{J}_{SC}$ is ill-conditioned when the iterations approach the solution. It is known that the speed of convergence of iterative methods depends on the spectral distribution of the matrix $\mathbf{J}_{SC}$. It was shown in [28] that the eigenvalues after appropriate preconditioning belong to a positive interval independent of the iteration and the condition number of the preconditioned matrix is bounded by a constant multiple of the condition number of $\mathbf{F}$.

6 Numerical experiments and Conclusion

The algorithms outlined in the previous sections were implemented in MATLAB (R2016a) on a Linux workstation with 3.00GHz clock frequency and 32 GB RAM. The test problem used is designed to illustrate the behavior of the algorithms more than to model an actual phenomena. We study, numerically, the following algorithms:

ALG1 ADMM Algorithm 2

ALG2 ADMM Algorithm 2 with Algorithm 4 as a solver for the Stokes problem with a slip/stick boundary condition (3.19).

ALG3 ADMM Algorithm 3

ADMM algorithms are very sensitive to the choice of the penalty parameter: the number of iterations (and consequently the computational cost) depends strongly on the choice of γ. A simple procedure for the choice of a penalty parameter is a uniform sampling of interval $(.1,\ \delta)$, $(\delta > 1)$. Fig. 1 shows, for ALG3, the number of iterations with respect to the penalty parameter γ, for $r = 3$ and $g = 0.01$. The "optimal" penalty parameter is $\gamma^* \approx 7$. After some sampling procedures, we found the following "optimal" values:

- $\gamma \approx 1$ and $\gamma_2 \approx 30$ (see [16]), for ALG1;
- $\gamma \approx 1$ for ALG2;
- $\gamma \approx 7$ for ALG3.

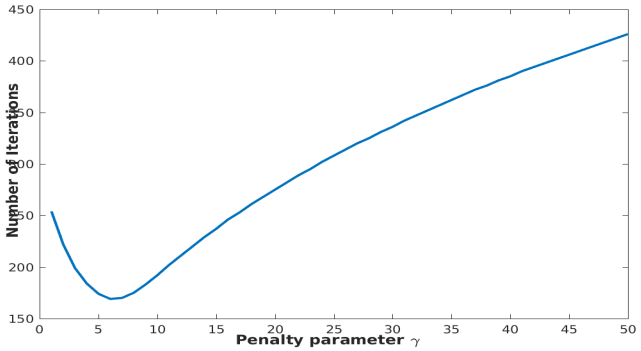

Figure 1: Number of iterations of ALG3 versus the penalty parameter for $r = 3$ and $g = 0.01$

The stopping criterion for the main loop of Algorithm 3 is the relative error on $\boldsymbol{s}^k := (\boldsymbol{u}^k, p^k, \mathbf{Z}^k)$, i.e.,

$$\| \boldsymbol{s}^k - \boldsymbol{s}^{k-1} \|_{L^2} < 10^{-5} \| \boldsymbol{s}^k \|_{L^2} \ .$$

To make sure that the ADMM algorithms converge, we also check that the residual of the constraints is sufficiently small, i.e.

$$\| \mathbf{Z}^k - D(\boldsymbol{u}^k) \|_{L^2} < 10^{-4} \quad \text{(for ALG2 and ALG3) and}$$
$$\| \phi^k - \boldsymbol{u}_\tau^k \|_{L^2} < 10^{-4} \quad \text{(for ALG1 and ALG3)} \ .$$

The tolerance for the inner solvers (Algorithm 1 and Algorithm 4) is set to 10^{-4}.

The main (numerical) advantage of ALG1, ALG2 and ALG3 is that the matrices involved do not change during the whole iterative process. A factorization is therefore done once and for all in the initialization step as follows.

- For ALG1 and ALG3, we use the symmetric indefinite factorization (MATLAB function `ldl`) with column/row permutations to reduce fill-in.
- For ALG2, we use the Cholesky factorization (MATLAB function `chol`) with column/row permutations to reduce fill-in.

Then in the rest of the iterative process, the linear systems reduce to forward/backward substitutions.

6.1 Driven cavity

This is classical example that has been studied by many authors (see [11, 13]) with classical Tresca's condition. Our threshold condition is different, and we would like to show by means of numerical simulations the existence of slipping/sticking zone. For that purpose, we consider the unit square $\Omega = (0,\ 1)^2$ and we assume that its boundary consists of two portions Γ_D and S defined as follows

$$\begin{aligned} \Gamma_D &= \{0\} \times (0,1) \cup (0,\ 1) \times \{0\} \\ S &= S_1 \cup S_2, \quad S_1 = (0,\ 1) \times \{1\} \text{ and } S_2 = \{1\} \times (0,\ 1). \end{aligned}$$

Let us consider

$$\begin{aligned} u_1(x,y) &= -x^2 y(x-1)(3y-2), \\ u_2(x,y) &= xy^2(y-1)(3x-2), \\ p(x,y) &= (2x-1)(2y-1). \end{aligned} \tag{6.1}$$

We adjust the right hand-side in (1.1) so that (6.1) is the exact solution of the problem (1.1)-(1.2). From the definition of $\boldsymbol{T}$ we deduce that

$$(\boldsymbol{Tn})_{\boldsymbol{\tau}} = 2\nu_0 |D(\boldsymbol{u})|^{r-2} \left[(D(\boldsymbol{u})\boldsymbol{n}) \cdot \boldsymbol{\tau}\right]\boldsymbol{\tau}\,.$$

Thus on S_1, for $\boldsymbol{n} = (0,1)^{\boldsymbol{T}}$ and $\boldsymbol{\tau} = (1,0)^{\boldsymbol{T}}$ we have

$$(\boldsymbol{Tn})_{\boldsymbol{\tau}} = -4\nu_0 x^2(x-1)\left[2x^2(3x-2)^2 + 8x^4(x-1)^2\right]^{(r-2)/2} \begin{bmatrix} 1 \\ 0 \end{bmatrix},$$

while on S_2, for $\boldsymbol{n} = (1,0)^{\boldsymbol{T}}$ and $\boldsymbol{\tau} = (0,-1)^{\boldsymbol{T}}$, we have

$$(\boldsymbol{Tn})_{\boldsymbol{\tau}} = -4\nu_0 y^2(y-1)\left[2y^2(3y-2)^2 + 8y^4(y-1)^2\right]^{(r-2)/2} \begin{bmatrix} 0 \\ -1 \end{bmatrix}.$$

Table 1 shows computed values of $\max\limits_{S}|(\boldsymbol{Tn})_{\boldsymbol{\tau}}|$ for various values of the parameter r.

r	1.5	2	3	3.5
$\max\limits_{S}\lvert(\boldsymbol{Tn})_{\boldsymbol{\tau}}\rvert$	0.074	0.048	0.026	0.022

Table 1: Computed $\max\limits_{S}|(\boldsymbol{Tn})_{\boldsymbol{\tau}}|$ for $\nu_0 = 0.04$, and various values of r

The streamlines plot represented in Figures 2–Figures 5 confirm the existence of slip/stick zone for values of r and g. It is observed from the figures below that for $\max\limits_{S}|(\boldsymbol{Tn})_{\boldsymbol{\tau}}| < g$, the solution of (1.1)–(1.7) is such that $\boldsymbol{u}_{\boldsymbol{\tau}}|_S = \boldsymbol{0}$. So no slip occurs on S. But the velocity $\boldsymbol{u} = (u_1, u_2)$ given by (6.1) is such that $\boldsymbol{u}_{\boldsymbol{\tau}}|_S \neq \boldsymbol{0}$. Therefore the solution of (1.1)–(1.7) with $\max\limits_{S}|(\boldsymbol{Tn})_{\boldsymbol{\tau}}| < g$ is different from the triplet (u_1, u_2, p) given by (6.1).
Next, it is noted from figures below that for $\max\limits_{S}|(\boldsymbol{Tn})_{\boldsymbol{\tau}}| > g$, the solution of (1.1)–(1.7) is such that $\boldsymbol{u}_{\boldsymbol{\tau}}|_S \neq \boldsymbol{0}$. Hence the non-trivial slip occurs.

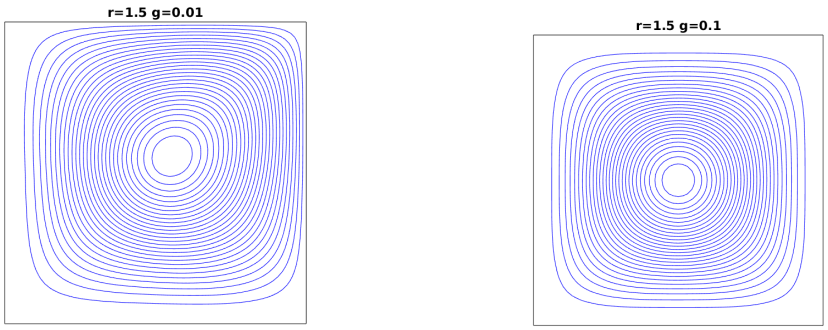

Figure 2: Streamlines plot for $r = 1.5$, $g = 0.01$ and $g = 0.1$

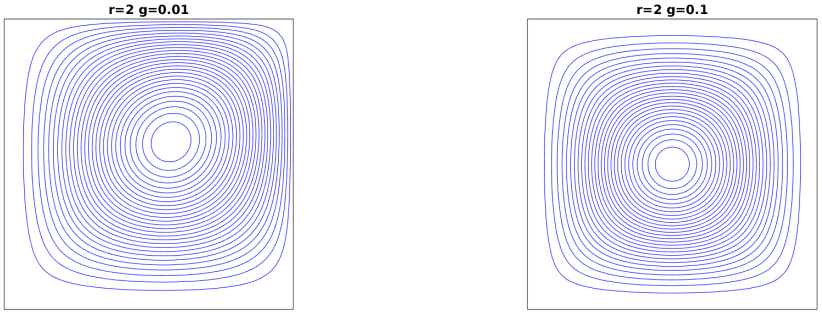

Figure 3: Streamlines plot for $r = 2$, $g = 0.01$ and $g = 0.1$

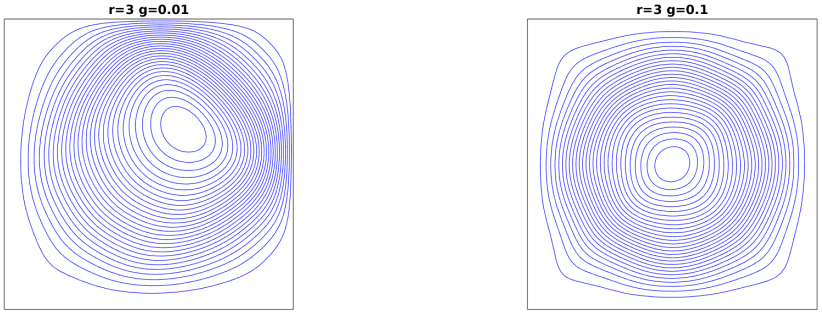

Figure 4: Streamlines plot for $r = 3$, $g = 0.01$ and $g = 0.1$

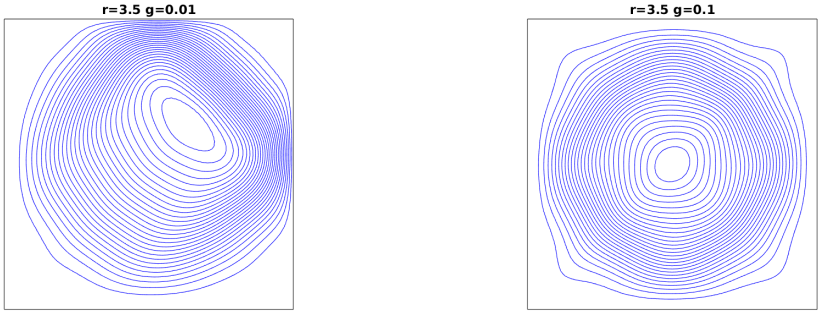

Figure 5: Streamlines plot for $r = 3.5$, $g = 0.01$ and $g = 0.1$

We report in Tables 2-5 the performances of ALG1 and ALG2 on the driven cavity problem. We first notice that, in the slip case ($g = 0.01$), ADMM algorithm with interior point solver (ALG2) requires less iterations for convergence than ALG1, for $r = 1.5,\ 2$. The interior point Algorithm 4 is more accurate in solving the Stokes problem with stick/slip boundary condition than the inner ADMM Algorithm 1. In terms of CPU time, ALG1 outperforms ALG2. For $r = 3,\ 3.5$ both algorithms are almost equivalent in terms of the number of iterations but ALG1 is far most efficient in terms of CPU time.
For the stick case ($g = 0.1$), both algorithms are equivalent in terms of the number of iterations required for convergence but ALG1 outperforms ALG2 in terms of CPU time.

Slip bound	$g = 0.01$				$g = 0.1$			
Algorithms	ALG1		ALG2		ALG1		ALG2	
Mesh size	IT	CPU	IT	CPU	IT	CPU	IT	CPU
1/16	101	0.3728	38	0.779	31	0.144	31	0.783
1/32	103	1.9108	39	1.791	31	0.318	30	1.840
1/64	103	10.1587	40	13.943	31	1.554	30	10.067
1/128	104	76.7018	46	116.625	31	11.053	30	157.000
1/256	104	571.6836	48	960.187	31	80.430	30	536.316

Table 2: Performances of ALG1 and ALG2 on the driven cavity problem with $r = 1.5$

Slip bound	$g = 0.01$				$g = 0.1$			
Algorithms	ALG1		ALG2		ALG1		ALG2	
Mesh size	IT	CPU	IT	CPU	IT	CPU	IT	CPU
1/16	128	0.331	70	0.928	49	0.081	49	0.783
1/32	131	2.282	64	3.500	48	0.444	48	2.154
1/64	132	12.088	60	23.056	49	2.189	49	14.261
1/128	132	90.903	65	160.356	50	15.541	50	217.826
1/256	132	679.84	67	1155.470	50	113.126	50	912.258

Table 3: Performances of ALG1 and ALG2 on the driven cavity problem with $r = 2$

Slip bound	$g = 0.01$				$g = 0.1$			
Algorithms	ALG1		ALG2		ALG1		ALG2	
Mesh size	IT	CPU	IT	CPU	IT	CPU	IT	CPU
1/16	171	0.411	213	11.223	271	0.402	271	2.059
1/32	210	3.260	224	49.347	261	2.032	262	6.643
1/64	228	17.619	260	418.081	263	9.541	263	42.845
1/128	232	122.97	244	2577.807	252	63.102	252	327.114
1/256	238	1008.123	***	¿ 10000	247	441.553	248	2258.399

Table 4: Performances of ALG1 and ALG2 on the driven cavity problem with $r = 3$

In Tables 6-7, we summarize the performances of ALG3 (ie. the second ADMM Algorithm 3). As expected, the number of iterations in the slip case is higher than the corresponding number with ALG1 and ALG2. In the stick case, ALG3 is almost equivalent to ALG1 and ALG2. In terms of CPU time, ALG3 outperforms ALG1 and ALG2. For the largest problem ($h = 1/256$) in slip mode, ALG3 is approximatively twice faster than ALG2.

Slip bound	$g = 0.01$				$g = 0.1$			
Algorithms	ALG1		ALG2		ALG1		ALG2	
Mesh size	IT	CPU	IT	CPU	IT	CPU	IT	CPU
1/16	224	0.532	303	17.696	402	0.666	403	2.936
1/32	291	4.037	314	73.476	415	3.301	416	10.180
1/64	318	21.845	309	511.751	401	14.795	401	61.979
1/128	341	169.235	379	4271.249	428	106.588	428	528.288
1/256	366	1297.112	***	¡10000	386	681.640	387	2737.125

Table 5: Performances of ALG1 and ALG2 on the driven cavity problem with $r = 3.5$

Slip bound	$g = 0.01$				$g = 0.1$			
	$r = 1.5$		$r = 2$		$r = 1.5$		$r = 2$	
Mesh size	IT	CPU	IT	CPU	IT	CPU	IT	CPU
1/16	171	0.296	211	0.312	31	0.126	49	0.224
1/32	174	1.252	215	1.612	31	0.233	48	0.336
1/64	174	5.820	215	7.038	32	1.097	49	1.642
1/128	175	40.916	216	49.766	31	7.316	50	11.603
1/256	175	290.658	216	356.370	31	51.711	50	82.965

Table 6: Performances of ALG3 on the driven cavity problem $r = 1.5$ and $r = 2$

Slip bound	$g = 0.01$				$g = 0.1$			
	$r = 3$		$r = 3.5$		$r = 3$		$r = 3.5$	
Mesh size	IT	CPU	IT	CPU	IT	CPU	IT	CPU
1/16	289	0.393	289	0.454	271	0.375	402	1.336
1/32	281	1.965	301	2.223	261	1.816	415	3.054
1/64	281	9.194	323	11.208	263	8.753	401	13.621
1/128	283	65.353	355	84.042	252	58.392	428	100.915
1/256	287	473.657	389	652.408	247	409.441	386	643.234

Table 7: Performances of ALG3 on the driven cavity problem for $r = 3$ and $r = 3.5$

6.2 Channel with a backward facing step

We now consider the numerical simulation of a nonlinear Stokes problem with stick/slip boundary condition in a two-dimensional channel with a backward facing step, as illustrated in Figure 6

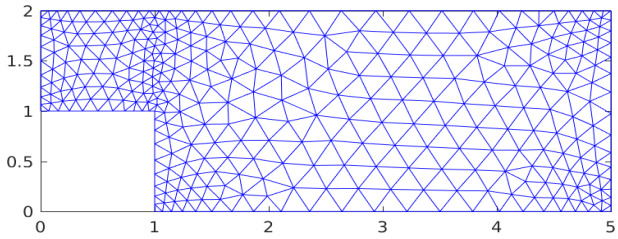

Figure 6: Mesh sample for the channel with backward step problem

We assume that the boundary is made of Γ_D and S with

- $S = S_1 \cup S_2 \cup S_3$, $S_1 = (0,\ 1) \times \{1\}$, $S_2 = \{1\} \times (0,\ 1)$ and $S_2 = (1,\ 5) \times \{0\}$ (the bottom)
- $\Gamma_D = \Gamma_1 \cup \Gamma_2 \cup \Gamma_3$, $\Gamma_1 = \{0\} \times (1,\ 2)$ (left boundary), $\Gamma_2 = (0,\ 5) \times \{2\}$ (top boundary) and $\Gamma_3 = \{5\} \times (0,\ 2)$ (right boundary).

The Dirichlet boundary conditions are

- $\boldsymbol{u} = ((y-1)(2-y), 0)$ on Γ_1,
- $\boldsymbol{u} = 0$ on $\Gamma_2 = (0,\ 5) \times \{2\}$,
- $\boldsymbol{u} = (y(2-y)/8, 0)$ on Γ_3.

Note that Γ_1 and Γ_3 are such that $\displaystyle\int_{\partial\Omega} \boldsymbol{u} \cdot \boldsymbol{n} d\sigma = 0$.

For this problem, we only consider ALG3 (ADMM Algorithm 3). We first consider a nonuniform mesh of the channel with 363 nodes and 625 triangles, obtained with KMG package ([39]). Figure 7 and Figure 8 show the streamlines of the flow for values of r and g. We notice that for $g = 0.01$, the flow is in slip mode on S.

To study the numerical behavior of ALG3, the initial mesh of Figure 6 is successively refined to produce meshes with 1350, 5199, 20397 and 80793 nodes. We summarize in Tables 8-9 the performances of ALG3. We first notice that the number of iterations is almost independent of the mesh size for $r = 1.5$ and $r = 2$. For $r = 3$ and $r = 3.5$ the number of iterations slightly varies from the smallest to the largest problems. Note that the penalty parameters are set once and for all for all values of r. Appropriate choice of the penalty parameters with respect to r may improve the results of ALG3.

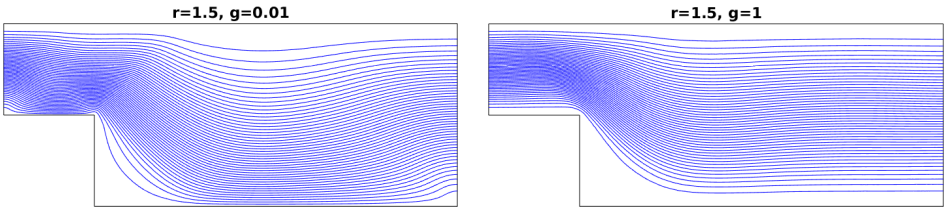

Figure 7: Streamlines plot for $r = 1.5$, $g = 0.01$ and $g = 1$

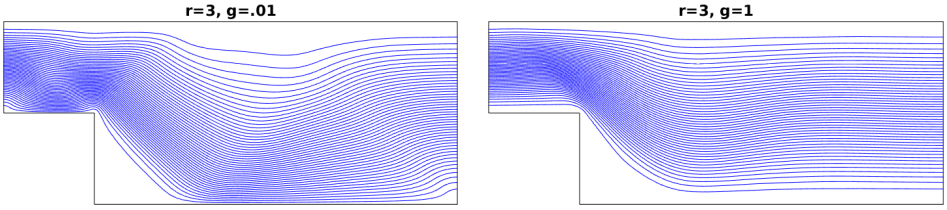

Figure 8: Streamlines plot for $r = 3$, $g = 0.01$ and $g = 1$

Slip bound	$g = 0.01$				$g = 1$			
	$r = 1.5$		$r = 2$		$r = 1.5$		$r = 2$	
Mesh nodes	IT	CPU	IT	CPU	IT	CPU	IT	CPU
363	168	0.417	202	0.450	148	0.380	173	0.386
1350	176	1.461	200	1.603	148	1.220	173	1.384
5199	172	6.506	200	7.333	148	5.572	172	6.296
20397	172	42.805	200	48.982	148	36.765	171	41.706
80793	173	301.007	199	342.909	148	256.802	172	294.306

Table 8: Performances of ALG3 for the channel with a backward facing step for $r = 1.5$ and $r = 2$

Slip bound	$g = 0.01$				$g = 1$			
	$r = 3$		$r = 3.5$		$r = 3$		$r = 3.5$	
Mesh nodes	IT	CPU	IT	CPU	IT	CPU	IT	CPU
363	254	0.565	260	0.615	222	0.488	234	0.551
1350	262	2.156	277	2.342	227	1.809	245	2.065
5199	276	10.111	306	11.712	232	8.513	268	10.249
20397	287	70.303	331	83.454	238	58.152	291	73.128
80793	294	506.894	345	604.586	241	414.843	306	534.543

Table 9: Performances of ALG3 for the channel with a backward facing step for $r = 3$ and $r = 3.5$

6.3 Concluding Remarks

We have constructed weak solution for the r-Laplacian Stokes equation under nonlinear slip boundary condition for $r \geq 2d(d+1)$. Next, we have formulated and investigated three numerical schemes for its finite element realization, these are in fact ADMM-type algorithms with different inner solver. It appears that the full ADMM Algorithm 3 leads to a significant saving of computational cost in the slip case. It also appears that for $r > 2$, the number of iterations of Algorithm 3 slightly depends on the mesh size. The construction of weak solution when $1 < r < 2d/(d+1)$ together with its complete numerical analysis is a future project. The fine tuning of the penalty parameter with respect to r is envisaged in a future work to make the algorithm virtually independent of the mesh size. Similarly, fine tuning (with respect to r) of parameters in the interior point Algorithm 4 may improve the ADMM Algorithm using interior point solver.

Acknowledgements. J. Koko acknowledges the hospitality of the University of Pretoria (Department of Mathematics) where this work was initiated and R. Kucera was financially supported by the project No. 17-01747S of the Czech Science Foundation and further by The Ministry of Education, Youth and Sports from the National Programme of Sustainability (NPS II) project "IT4Innovations excellence in science- LQ1602".
We are grateful to the comments and suggestions of the referees which have contributed to improve this study.

References

[1] V. Girault, and P.A. Raviart, *Finite Element Methods for Navier-Stokes Equations: Theory and Algorithms*, Springer-Verlag, Berlin-Heidelberg, 1986.

[2] C. Le Roux, Steady Stokes flows with threshold slip boundary conditions, *Math. Models Methods Appl. Sci.*, **15**, No 8, 1141-1168, 2005.

[3] A. Fortin, A.D. Cote and P.A. Tanguy, On the imposition of friction boundary conditions for the numerical simulation of Bingham fluid flows, *Comput. Meth. Appl. Mech. Engrg.*, **88**, 97-109,1991.

[4] R. R. Huilgol, A variational principle and variational inequality for a yield stress fluid in the pressence of slip, *J. Non-Newtonian Fluid Mech.*, **75**, 231-251, 1998.

[5] J. L. Lions., *Quelques Méthodes de Résolution des Problèmes aux Limites Non Linéaires*, Dunod, Paris, 1969.

[6] G. Duvaut, and J.-L. Lions, *Inequalities in Mechanics and Physics.* Grundlehren der Mathematischen Wissenschaften, **219**, Springer-Verlag, Berlin, 1976.

[7] H. Fujita, A mathematical analysis of motions of viscous incompressible fluid under leak or slip boundary conditions. *Mathematical Fluid Mechanics and Modeling (Kyoto, 1994)*, RIMS Kōkyūroko, **888**, Kyoto University, Kyoto, 199-216, 1994.

[8] H. Fujita & H. Kawarada. Variational inequalities for the Stokes equation with boundary conditions of friction type. In *Recent development in domain decomposition methods and flow problems*, Gakuto International series of Mathematical sciences and its applications, **vol** 11, 15–33, 1998.

[9] Yuan Li & Katai Li. Semi-discrete finite element methods for Navier-Stokes equations with nonlinear slip boundary conditions based on regularization procedure. *Numer. Math*, **117**, 1-36, 2011.

[10] M. Ayadi, L. Baffico, M. K. Gdoura & T. Sassi. Error estimates for Stokes problem with tresca friction conditions. *Esaim: M2AN* **48**, 1413–1429, 2014.

[11] T. Kashiwabara. On a finite element approximation of the Stokes equations under a slip boundary condition of the friction type. *J. Indust. Appl. Math*, **30**, 227–261, 2013.

[12] T. Kashiwabara. On a strong solution of the non stationary Navier Stokes equations under lip or leak boundary conditions. *J. Differ. Equ.*, **254**, 756-778, 2013.

[13] Y. Li and R. An. Penalty finite element method for Navier-Stokes equations with nonlinear slip boundary conditions. *Int. J. Numer. Methods Fluids.*, **69**, 550-566, 2011.

[14] Y. Li & K. Li. Penalty finite element method for Stokes problem with nonlinear slip boundary conditions. *Appl. Math. Comput*, **204**, 216-226, 2008.

[15] J.K. Djoko & M. Mbehou, Finite element analysis for Stokes and Navier Stokes equations driven by threshold slip boundary conditions. *Int. J. Numer. Anal. Model. Ser. B*, 4:235-255, 2013.

[16] J.K. Djoko & J. Koko, Numerical method for the Stokes and Navier-Stokes equations driven by threshold slip boundary conditions. *Comput. Methods Appl. Mech. Engrg* **305**, 936-958, 2016.

[17] J.K. Djoko & M. Mbehou, Finite element analysis of the stationary power law Stokes equations driven by friction boundary conditions. *J. Numer. Math.*, **23**, No 1, 21-40, 2015.

[18] R. Glowinski and A. Marrocco, Sur l'approximation, par elements finis d'ordre un, et la resolution par penalisation-dualite, d'une classe de problemes de Dirichlet nonlineaires. *RAIRO*, Serie Rouge, Analyse Numerique, **9**, 41-76, 1975.

[19] J. Baranger, P. Georget, & K. Najib, Error estimates for a mixed finite element method for a non-Newtonian flow. *J. Non-Newtonian Fluid Mech.*, **23**, 415-421, 1987.

[20] J. Baranger, K. Najib, Analyse numerique des ecoulements quasi-newtoniens dont la viscosité obéit à la loi de puissance ou la loi de Carreau. *Numer. Math.*, vol 58, 35–49, 1990.

[21] D. Sandri., Sur l' approximation numerique des ecoulements quasi-newtoniens dont la viscosité obéit à la loi de puissance ou la loi de Carreau. *M2AN.*, **27**, No 2, 131-155, 1993.

[22] J.S. Howell, Dual-mixed finiteelement approximation of Stokes and nonlinear Stokes problems using trace-free velocity gradients. *J. Comput. Appl. Math.*, **231**, 780-792, 2009.

[23] John W. Barrett & W.B. Liu, Finite element error analysis of a quasi-Newtonian flow obeying the Carreau or power law. *Numer. Math.*, **64**, 433-453, 1993.

[24] John W. Barrett & W. B. Liu., Finite element approximation of the p-Laplacian. *Math. Comp.*, **61**, 523-537, 1993.

[25] S. S. Chow, Finite element error estimates for non-linear elliptic equations of monotone type. *Numer. Math.*, **54**, 373-393, 1989.

[26] R. Glowinski, *Finite element methods for incompressible viscous flow.* In Handbook of Numerical Analysis, P.G Ciarlet and J.L Lions, eds, vol. IX, North Holland; Amsterdam, 3–1176, 2003.

[27] R. Glowinski, *Numerical Methods for Nonlinear Variational Problems.* Springer Series in Computational Physics, Springer-Verlag, Berlin Heidelberg, 2008.

[28] R. Kučera, J. Machalová, H. Netuka, and P. Ženčák, An interior point algorithm for the minimization arising from 3D contact problems with friction. *Optim. Method Softw.*, 6(28):1195–1217, 2013.

[29] R.A. Adams, *Sobolev Spaces*, Academic Press, New York, 1975.

[30] H. Brezis, *Functional Analysis, Sobolev Spaces and Partial Differential Equations.* Springer, New York, 2010.

[31] R. Temam, *Navier Stokes equations: Theory and Numerical Analysis.* 2nd ed., AMS Chelsea publishing, 2001.

[32] R. Glowinski and P. Le Tallec, *Augmented Lagrangian and Operator-Splitting Methods in Nonlinear Mechanics*, SIAM, Philadelphia, 1989.

[33] N. Kikuchi, and J.T. Oden, *Contact Problems in Elasticity*, SIAM, Philadelphia, 1988.

[34] W. Han, and B.D. Reddy, *Plasticity Mathematical theory and numerical analysis.* Second edition. Interdisciplinary Applied Mathematics 9, Springer, New York, 2013.

[35] S. Wirght, *Primal-Dual Interior Point Methods*, SIAM, Philadelphia, 1997.

[36] R. Kučera, J. Haslinger, V. Šátek, and M. Jarošová, Efficient methods for solving the Stokes problem with slip boundary conditions, *Math. and Comput. Simul.*, submitted 2015.

[37] J. Nocedal, A. Wächter, and R. A. Waltz, Adaptive barrier strategies for nonlinear interior methods. *TR RC 23563, IBM T.J. Watson Research Center*, 2005.

[38] M. Jarošová, R. Kučera, and V. Šátek, A new variant of the path-following algorithm for the parallel solving of the Stokes problem with friction. In P. Iványi and B. H. V. Topping, editors, *Proceedings of the Fourth International Conference on Parallel, Distributed, Grid and Cloud Computing for Engineering*, Stirlingshire, UK, 2015. Civil-Comp Press, Paper 11.

[39] J. Koko, A MATLAB mesh generator for two-dimensional finite element methd. *Appl. Math. Comput.*, **250**, 650-664, 2015.